ENGINEERING DESIGN FILE

Project File Number: Environmental Restoration WAG 5

Project/Task: WAG 5 Comprehensive RI/FS

Subtask: Operable Unit 5-12, Sites ARA-23 and ARA-24

Title: IN SITU GAMMA RADIATION SURVEY AT ARA-23 AND ARA-24

Summary:

This EDF presents the results of an in situ radiation survey that was conducted at two WAG 5 sites, ARA-23 and ARA-24. These surveys were conducted as part of the Operable Unit 5-12 Remedial Investigation/Feasibility Study and were to measure and determine the detailed distribution and concentration of Cs-137 in the surface soil.

ARA-23 is a large windblown soil contamination area surrounding both the ARA-I and ARA-II facilities. This contamination was a result of the SL-1 accident and its subsequent cleanup activities. ARA-24 is a windblown contamination area resulting from the reactor operations at the ARA-III facility.

The INEEL Environmental Monitoring personnel using a vehicle-mounted scillinator with a GPRS system successfully completed the ARA-23 and ARA-24 in situ radiation surveys. Over 69,000 measurements were collected at ARA-23 and over 13,000 measurements were collected at ARA-24. These data were converted to estimates of in situ Cs-137 concentrations based on methods developed and adapted by INEEL radiation measurements personnel. Converted data were compiled into maps showing the quantitative distribution of Cs-137 across these sites.

Distribution (complete package): Frank L. Webber, Chris M. Hiaring

Distribution (summary package only):

Author	Dept.	Reviewed	Date	Approved	Date
Nick Josten	4160	C. M. Hiaring	10/28/97	F. L. Webber	10/28/97
		LMITCO Review Chris M Hiaring	Date 10/28/97	LMITCO Approval Frank L Webber	Date 10/28/97

RESULTS OF THE IN SITU GAMMA RADIATION SURVEY AT ARA-23 AND 24

INTRODUCTION

This report summarizes the in situ radiation survey conducted at the Auxiliary Reactor Area (ARA)-23 and ARA-24 sites during July through September, 1997 as part of the Waste Area Group (WAG) 5, Operating Unit 5-12 (OU 5-12) Remedial Investigation/Feasibility Study (RI/FS). The specific purpose of the investigation was to determine the detailed distribution and concentration of Cs-137 soil contamination at the ARA-23 and ARA-24 sites. This investigation supports the Comprehensive Environmental Response, Compensation and Liability Act (CERCLA) activities at Idaho National Engineering and Environmental Laboratory (INEEL), as implemented under the Federal Facility Agreement/Consent Order (FFA/CO).

BACKGROUND

The ARA facilities, originally called the Army Reactor Area, were constructed in the 1950s to support of the Army Nuclear Program. The Army program was phased out in the early 1960s, and the group of facilities became the Auxiliary Reactor Area in 1965. Since then, all the reactors have been removed from the ARA facilities. From 1966 to 1989, work at ARA included a variety of technical support services for INEEL research and development programs that used the metallurgy laboratory, instrument development laboratory, or the hot cell facility. There have been no active operations conducted at ARA since 1989. Decontamination and decommissioning of the ARA-I/II and ARA-III facilities is currently in progress.

The ARA-23 site is a large area of primarily windblown contamination around the ARA-I and ARA-II facilities that resulted from the SL-1 reactor accident in 1961 at ARA-II. During this accident, the reactor vessel and building were severely damaged and highly contaminated. Much of the contamination still detected around the ARA-I/II facilities was disseminated either during the accident or the subsequent massive cleanup effort of the reactor and building structure. Although the accident occurred within the ARA-II facility, portions of the ARA-I facility were contaminated because it was used as a staging and operations area for the cleanup effort. Transport of debris to the SL-1 burial ground, located approximately 1600 feet northeast of the reactor site, also spread contamination in the area. The contamination is believed to be generally limited to the upper few inches of surface soils. The ARA-23 boundary encompasses more than 240 acres, of which approximately 40 acres were selected for additional characterization based on a 1990 aerial radiation survey and on interpolation of widespread sampling results.

The ARA-24 site encompasses all of the potentially contaminated surface soils associated with ARA-III facility, excluding the ARA-12 site. The surface soil contamination at the ARA-III

facility most likely originated from the process and ventilation stacks at the facility. The Army Gas Cooled Reactor Experiments were conducted from 1959 to 1961 at ARA-III. Then the facility was converted to support the Mobile Low Power Reactor tests conducted at ARA-IV until 1965. Support structures, including laboratories and office space were utilized until the facility was shut down in 1989. The ARA-12 evaporation pond is also located nearby. The total area is approximately 10 acres and extends outward from the facility, primarily to the northeast.

Cs-137 has been chosen as the indicator radionuclide at both ARA-23 and ARA-24 because it is known to be widespread and because its 662 keV gamma-ray is readily detected by field screening equipment. Sr-90 also occurs widely at these sites and is equally important from a risk assessment standpoint. However, as a pure beta emitter, Sr-90 is more difficult to detect using field screening methods. Previous WAG 5 studies show that Cs-137 and Sr-90 are co-located, suggesting that Cs-137 may be a valid qualitative indicator for Sr-90 distribution. However, during the SL-1 cleanup, Sr-90 was found beyond the limits of the Cs-137 distribution, which indicates that their co-location may not be universal. For the purposes of this report, it must be emphasized that the analysis herein applies strictly to Cs-137 on the assertion that all detected gamma radiation above background is derived from Cs-137 decay. Any connection with Sr-90 distribution and concentration must be established independently.

INVESTIGATION OBJECTIVES

The OU 5-12 RI/FS Work Plan (DOE/ID-10555) identifies the horizontal and vertical extent of the Cs-137 contamination at the ARA-23 and ARA-24 sites as data gaps. The work plan calls for the soils to be sampled in three phases: 1) a sodium iodide detector field survey for gamma radiation; 2) statistical analysis of field results and laboratory gamma spectroscopy results; and 3) ranked-set sampling as described in the Field Sampling Plan (Appendix D of the work plan), if required by the results of 1 and 2. This report presents the results of the Phase 1 Gamma Radiation Survey.

A specific objective of the work plan is to define the extent of the Cs-137 soil contamination that exceeds 17 pCi/g. The 17 pCi/g limit is based on the residential exposure scenario assumed to begin 100 years in the future after the mandatory institutional control period has expired. The results of this Phase 1 Gamma Radiation Survey will be evaluated by the regulatory agencies and DOE. Future decisions regarding remedial activities at the ARA-23 and ARA-24 sites will be based on this study in conjunction with soil sample results, data quality and usability, process knowledge, and other information available to decision makers. Potential applications of this analysis include:

1) defining further characterization activities,

2) defining an interim action or housekeeping activity,

3) providing data for the WAG 5 BRA and the FS alternative development,

4) improved estimates of contaminated material volume, and

5) providing the framework for future remedial actions under the WAG 5 comprehensive Remedial Action/Remedial Design phase.

METHOD

The in situ gamma radiation survey involves measuring gamma radiation from a position above the contaminated soil surface. Figure 1 shows the typical measurement geometry for an in situ gamma-ray detector. Radionuclides within the soil emit photons. The soil dissipates photon energy through absorption and scattering processes, but some energy escapes the soil zone and radiates outward to interact with the gamma-ray detector. The detector "counts" these interactions to give a measure of the radioactivity present. The number of gamma rays "counted" at a given measurement point depends on several factors as listed in Table 1. The factor G contains the desired information on radionuclide concentrations.

Table 1. *Factors affecting in situ measurement of radionuclides*

Symbol	Factor
Ω	sensor field of view
ρ	soil density
γ	gamma-ray energy
E	detector efficiency
G	amount and distribution of radionuclide in soil

Equipment

One of the distinct advantages of in situ measurement relates to the sensor field of view. The field of view may be made quite large through appropriate sensor design, permitting the detector to count photons emitted over an extended area. Thus, even for low radionuclide concentrations, a large number of photon-detector interactions occur and the measurement may be made rapidly, e.g. in one second. At this speed it becomes possible to fully map radionuclide concentrations over a large area by attaching the detector to a mobile system and traversing the area of interest.

The ARA-23 and ARA-24 areas were mapped using two types of in situ detectors: the INEEL Environmental Monitoring Global Positioning Radiometric Scanner (GPRS) and a portable Germanium spectrometer (Ge-spectrometer). The GPRS consists of a large area plastic scintillation detector mounted on the front of a HumVee all-terrain vehicle equipped with global positioning navigation instruments. The scintillation detector is permanently mounted to

maintain a constant detector-to-ground distance of 1 meter. At this elevation, the scintillation detector has an approximately 25 feet diameter field of view.

Ge-spectrometer measurements were collected in areas inaccessible to the GPRS and at a selected set of calibration points. During a standard in situ measurement, the Ge-spectrometer sets on a tripod that maintains a constant detector-to-ground distance of 1 meter. At this elevation the Ge-spectrometer has approximately the same field of view as the scintillation detector, i.e. about 25 feet in diameter. Measurement locations are determined separately through conventional surveying techniques. Several auxiliary Ge-spectrometer measurements were made using an alternate measurement geometry. These will be described in a later section.

Calibration

In situ Ge-spectrometer measurements have been routinely conducted for many years and the protocol for converting raw count data to radionuclide concentration estimates is well developed. Attachment 1 contains details of the conversion process used for the Ge-spectrometer measurements at ARA-23. The method employed in these calculations assumes that the radionuclide (Cs-137) is distributed in an exponentially decreasing fashion, decreasing from A_{max} at the surface to A_{max}/e at a depth of 4-inches (e=2.718). The analysis software reports the value A_{max} at each Ge-spectrometer measurement location.

Each 1 to 2 seconds, the GPRS generates a "count" value that reflects the bulk radionuclide concentration throughout the sensor field of view, which is approximately 25 feet in diameter. Successive measurements occur as the field of view is swept over the ground surface by motion of the GPRS vehicle. Count values change in response to the spatial distribution of radionuclides in the soil. These data are quantitative in the sense that they accurately depict relative radionuclide concentration as it varies across a site. However, absolute concentration estimates can be made only after calibrating the detector. The calibration process accounts for the influence of the first four factors in Table 1 above. With these factors known, the raw count data may be interpreted in terms of the remaining factor, G, which gives an estimate of the absolute radionuclide concentration.

Two separate calibration approaches were used in the ARA surveys. Both methods require that background radiation arising from natural radionuclides be removed from raw count data prior to conversion. Background analysis is discussed in some detail below. Both calibration methods also assume constant soil density and gamma-ray energy. Specifically, the density 1.5 g/cm^3 is assumed for shallow, unconsolidated root zone soils. Secondly, since Cs-137 is the dominant gamma-ray emitting radionuclide at the ARA sites, gamma-ray energy is taken to be 662 keV only, which is the energy of the single gamma-ray generated during Cs-137 decay.

In the first calibration method, a Monte Carlo simulation and geometric arguments were employed to establish sensor field of view, and detector efficiency. Attachment 2 contains details of the calculations. Several items are to be noted. First, field of view and detector efficiency factors are not based on direct measurements using the GPRS scintillator. Instead,

they are based on measurements made using a similar scintillator, where geometric arguments are employed to account for differences in detector size and shielding. Second, the final conversion factor contains some uncertainty that arises from uncertainty in the scintillation detector low-level discriminator setting. In this report, GPRS data are converted based on a mid-range estimate for this setting. Third, in determining G, which gives information on both the amount and distribution of Cs-137, it is necessary to assume a distribution in order to estimate amount. Attachment 1 calculations assume uniform Cs-137 to a depth of 4-inches. In this case, the final conversion factor assumes no Cs-137 occurs below this depth. A similar set of calculations (Attachment 3) provides conversion factors for uniform distributions to 1 inch and 2 inches.

The second GPRS calibration method utilizes a 14-point Ge-spectrometer calibration profile collected within the GPRS survey area. Cs-137 concentrations along this profile are computed from the Ge-spectrometer data in the normal fashion. Then, by forming an appropriate mathematical relationship between these computed concentrations and the GPRS data along the same profile, it is possible to determine a background value and conversion factor that fits one data set to the other. When the remaining GPRS data are converted using this calibration factor, they yield concentration values consistent with the same exponentially decreasing function as defined for the Ge-spectrometer calibration profile, i.e. 1/e decrease over 4-inches.

ARA-23 RESULTS

The results of the ARA-23 site in situ gamma radiation survey are presented in the following section. Preliminary areas of interest at ARA-23 were identified based on previous soil sample results. The in situ surveys were undertaken to further refine the details of contaminant distribution. Original survey specifications proposed data collection throughout the areas of interest at 25 feet nominal profile spacing, at an average speed of 2.5 mph, and with a data acquisition interval of approximately 2 seconds.

Data collection

Figure 2 shows the in situ gamma radiation survey data collection pattern for the ARA-23 area with the original survey boundary noted. The ARA-23 in situ gamma radiation survey was expanded to include several areas outside the original boundary based on preliminary results. Additional data were also collected adjacent to the SL-1 Burial Ground, northeast of the preliminary boundary. Finally, several profiles were collected in a radial pattern outward from the main site to assist with background evaluation. In total, over 69,000 in situ gamma radiation measurements were collected along the black track lines in Figure 2. The map also notes areas that were temporarily inaccessible to the GPRS vehicle.

The yellow-filled circles in Figure 2 show the locations of the in situ Ge-spectrometer measurements. Eighty-eight Ge-spectrometer measurements were collected from a rocky, debris-filled zone that was inaccessible to the GPRS vehicle. A second set of measurements were taken along the Ge-spectrometer calibration profile noted in the section above.

Bulk gamma-ray fields and background analysis

Figure 3 shows a color intensity map depicting the bulk gamma radiation measured by the GPRS system. On this map, uncolored areas correspond with locations that are greater than 25 feet from a measurement point. In the remaining areas, color indicates the gamma-ray field intensity in counts per second (cps) according to the scale indicated by the color bar. The maximum cps value recorded anywhere was 117,961 cps. The highest gamma radiation measurements recorded were located in four distinct areas; adjacent to the old ARA reactor facilities; immediately northeast of the old ARA reactor facilities; around the northeast boundary of the SL-1 Burial Ground; and along the dirt road between the ARA facilities and the SL-1Burial Ground. The lowest gamma radiation measurements were recorded at the survey fringes and along several of the radial background profiles. Intermediate values were obtained both southwest and northeast of the reactor facilities all the way to the survey boundary. The northeast trending pattern of elevated gamma radiation is more extensive than the pattern to the southwest. The northeast trending pattern of elevated gamma radiation is also characterized by a sharp boundary on its southeast margin and a very gradual boundary on its northwest margin. This zone correlates with the prevailing wind direction at the site.

In Figure 4, the same bulk gamma radiation data are presented with a color scale intended to highlight variations in the background gamma radiation field. The RESL soil samples (circles) and WAG 5 soil samples (triangles) have been included with their Cs-137 concentrations posted in pCi/g. One can estimate local background radiation by examining cps measurements in areas adjacent to low Cs-137 results (~1 pCi/g) in the soil samples. By this method, background appears to vary mostly within the range from 1200 to 1400 cps. The observed variation probably reflects natural variations in soil chemistry, density and vegetation. A value of 1300 cps was chosen as a best estimate, in part based on results of the Ge-spectrometer calibration discussed below.

Note also the very low background gamma radiation (<1000 cps) measured adjacent to the southwest corner of the SL-1 Burial Ground. This area was disturbed during the construction of the burial ground and now contains non-native soils with relatively low natural radioactivity. In addition to illustrating the tremendous sensitivity of the GPRS equipment, this scenario illustrates the effect of human activity on background variability. Survey planning must include a set of measurements specifically designed to characterize natural background variability, identify non-representative background areas and avert selection of a biased background radiation level.

Conversion to activity concentration

Figure 5 shows data along the Ge-spectrometer calibration profile (see Figure 2). In this chart, continuous GPRS data in cps are shown in blue. The red profile presents the Ge-spectrometer data results (in pCi/g) using the 4-inch exponential distribution model.

The relationship between the GPRS count data and the Ge-spectrometer data may be written as;

$C = (cps - bg) * K$ where:

C = Cs-137 concentration based on the 4-inch exponential model,

cps = raw count data from the GPRS scintillator,

bg = the background count rate, and

K = a linear conversion factor that scales cps to pCi/g.

These data were entered into a spreadsheet that permitted iteration of the factors bg and K to obtain a fit between the two data sets. Figure 6 shows the results from this procedure, where the values bg = 1300 cps and K = .019 (pCi/g)/cps have been determined. The background value falls near the middle of the observed background range and has been adopted as the best value for conversion of the GPRS data for all distribution models.

Table 2 summarizes the conversion factors developed for converting GPRS count values to Cs-137 concentrations in pCi/g at ARA-23. Each set of factors corresponds to a different assumption regarding the distribution of Cs-137 within the soil. Since the distribution model can affect the quantification process by as much as a factor of 2.5, it should be chosen based on supporting information if at all possible.

Table 2. *Conversion factors for GPRS data collected at ARA-23.*

Cs-137 Distribution Model	K (pCi/g)/cps	Background (cps)	Calibration Method
4-inch uniform	0.0091	1300	theoretical
2 inch uniform	0.0136	1300	theoretical
1 inch uniform	0.0228	1300	theoretical
4-inch exponential*	0.019	1300	direct measurement

* Graphics depicting results from the 4-inch exponential model (Figures 6 and 10) show Cs-137 concentrations *at the ground surface* ; it is understood that concentration decreases exponentially from this maximum value.

GPRS count data were converted to Cs-137 concentrations based on each set of conversion factors given in Table 2. Figures 7 through 10 present these results. The colored circles in Figure 10 show concentration values generated from Ge-spectrometer data as well, since these values are based on the same 4-inch exponential distribution model. Circle coloring uses the same concentration scale as for the main body of GPRS data. Note in particular the close fit between the GPRS data and the Ge-spectrometer calibration line. This is an expected result since these points were used to tie the two data sets together (see Figure 6).

Discussion of distribution models

The appropriate selection of a Cs-137 distribution model is critical at ARA since DOE may potentially remediate the ARA-23 site to a specific cleanup level. Preliminary negotiations between the stakeholders indicate that the cleanup level may be 17 pCi/g. Figure 11 illustrates the Cs-137 distribution model's effect on the size of a potential cleanup operation aimed at removing all soils above 17 pCi/g. The color coded outlines on Figure 11 show the boundary between Cs-137 exceeding 17 pCi/g (interior) in soil and Cs-137 less than 17 pCi/g (exterior) in soil. An approximate comparison in the acreage and volume of cleanup for the different models is given in Table 3. These calculations reflect soil areas within the originally defined ARA-23 survey boundary only. The volume estimates do not reflect construction equipment limitations, vegetation removal complications, or potential cross contamination during excavation. These may significantly increase soil volume estimates if a removal option is selected.

Table 3. Area and volume estimates for ARA-23 cleanup using different distribution models.

Description	Area (acres)	Cleanup Volume (cu yds)
survey boundary	39.2	-
>17 pCi/g Cs-137 to 1 inch depth	30.6	4097
>17 pCi/g Cs-137 to 2 inch depth	23.0	6188
>17 pCi/g Cs-137 to 4-inch depth	14.5	7793

It is important to note that uncertainty in radionuclide depth distribution is not unique to in situ radiation measurement techniques. The most common method for estimating radionuclide concentration, soil sampling, possesses the same inherent uncertainty. Normal soil sampling activities require that a soil core be taken to a specified depth. The core is then homogenized, its radioactivity is counted, and the result is divided into the mass of the core to provide a concentration value in pCi/g. This method will underestimate the maximum concentration in the core unless the core has truly uniform radionuclide distribution. The problem can only be averted by subdividing the core into discrete depth intervals and counting them separately, which is a difficult and expensive operation to perform in unconsolidated soil.

In situ measurement techniques include methods for addressing the depth distribution of radionuclides in some cases. In the case of Cs-137, a K x-ray emitted in the Cs-137 decay chain permits a comparison of attenuation between photons having very different energies. The K x-ray and the 662 keV gamma ray are emitted in known ratios. The relative numbers of each photon that escape the soil and are detected by a Ge-spectrometer give an indication of the depth from which they arise. For a deep soil source, virtually no K x-rays escape the shielding effect of the soil while gamma-rays are still detected. From a surface source, K x-rays and gamma-rays are detected in very nearly the proportion they are emitted.

A special set of Ge-spectrometer measurements were collected to evaluate depth distribution. These measurements were made along the Ge-spectrometer calibration profile using a detector height of six inches. These measurements showed K x-ray/662 keV gamma-ray peak ratios ranging between 0.15 and 0.25, with an average near 0.20. Table 4 below gives theoretical K x-ray/662 keV gamma-ray peak ratios for various depth distributions (see also Attachment 4). The average measured peak ratio is consistent with a uniform distribution to about 1 inch. This analysis also strongly indicates that the Cs-137 contamination begins very near the ground surface and is not overlain (and therefore shielded) by any significant amount of clean soil. These conclusions apply strictly to the windblown portion of the ARA-23 contamination plume where the calibration measurements were made.

Table 4. *X/gamma ratios for Cs-137 at different depth distribution.*

Source Uniform Down to (in)	Theoretical x/gamma ratio
0.5	0.32
0.7	0.26
0.9	0.21
1.2	0.17
6.0	0.077

A truly uniform distribution of Cs-137 throughout any depth is, of course, highly unlikely. Wind-deposited contamination that has been reworked by percolating groundwater might exhibit more of an exponentially or linearly decreasing concentration-depth profile. Attachment 4 gives a theoretical x/gamma peak ratio of 0.25 for Cs-137 concentrations that decrease linearly to a depth of 1.1 inch, which is at the maximum of the observed range. The distinction between the linear and uniform case cannot be made with any certainty. In fact, different distributions are very likely to occur in the various distinct settings such as the undisturbed desert, roadways or the rock piles.

Recent samples collected on the perimeter of the ARA-23 boundary support the thin contamination layer model. These samples were segregated into two depth intervals, 0 - 6 inches and 6 - 24-inches. Results have not yet been thoroughly analyzed, but they clearly show a marked decrease in Cs-137 soil concentrations below 6 inches.

Comparison between in situ methods and sampling

Figure 12 shows a summary of Cs-137 concentration data, including the GPRS data converted, using the 1 inch uniform distribution model, Ge-spectrometer data for the rock pile area converted to a 1 inch exponential distribution model, and sampling results based on 6-inch cores. Each data set has been plotted using an identical color scheme as shown by the color bar.

The Ge-spectrometer data for the rock pile show a clear continuation of the concentration trend observed for the main Cs-137 plume to the northeast, although a slight discontinuity and trend

variation is observed at the northeast boundary between the two data sets. A more pronounced discontinuity occurs at the southwest boundary. Here, the rock pile data reveal a broad concentration gradient adjacent to much lower, more uniform concentrations indicated by the GPRS data. The discontinuous boundaries may be due in part to the Ge-spectrometer analysis model which cannot account for the uneven rocky surface in the rock pile area and which may overestimate the depth extent of Cs-137. It is also quite reasonable to expect a difference in Cs-137 distribution between these areas due to differences in environmental processes and human activities over many years.

Soil sample data corroborate the general trends and concentration estimates determined from the in situ gamma radiation measurements. Figure 13 shows the quantitative comparison between the in situ gamma radiation survey estimates and sampling results in greater detail. The soil sample data in Figure 13 have been arranged in order of increasing concentration. The soil samples and in situ gamma radiation estimates follow the same general trend up to about 25 pCi/g. Some exceptions occur, primarily in the older RESL soil samples which tend to report Cs-137 concentrations greater than the in situ gamma radiation survey data. The WAG 5 soil samples agree more closely with the in situ gamma radiation survey data but tend to report lower concentration than the in situ survey data. Consistently low values from soil sample results may reflect the averaging that occurs when sample cores extend into relatively clean soils beneath the main layer of contamination.

The two data sets become erratic when the Cs-137 concentration exceeds 25 pCi/g. One explanation for this phenomenon is that the high level Cs-137 contamination is heterogeneous on a relatively fine scale, i.e. much of the radioactivity emanates from a small percentage of soil particles spaced some finite distance apart within the contaminated zone. The sample cores, which are only an inch or so in diameter, can produce highly fluctuating results depending on whether a sample location coincides with one or more hot particles. The in situ method, which averages Cs-137 activity over a 25 feet diameter, does not exhibit these erratic fluctuations. The key factor in determining whether a measurement method will produce erratic results or smooth results is the scale of the Cs-137 heterogeneity compared with the scale of the measurement method. If this hypothesis is correct, the ARA-23 data suggest that Cs-137 heterogeneity occurs on a scale greater than an inch and less than 25 feet, at least in the areas of elevated radioactivity. It is not clear why this phenomenon is observed only in the areas of elevated radiation. Cs-137 particles may be distributed on a finer scale in the low radioactivity areas located away from the reactor site. It is reasonable to expect that the scale of particle heterogeneity depends on the mechanism of Cs-137 deposition, e.g. windblown, air fallout, groundwater transport, etc. If true, measurement of this scale may prove useful for evaluating the history of soil contamination sites. This heterogeneity may not be significant if it occurs at concentration above the cleanup limit.

UNCERTAINTY CONSIDERATIONS

Concentration uncertainty caused by the unknown Cs-137 depth distribution has been discussed already in detail. Two other sources of uncertainty require some additional treatment here.

Attachment 1 states that the precise value of the low-level discriminator for the GPRS scintillator is unknown and that this leads to a +40% to -20% uncertainty in the calculated conversion factor for the uniform distribution model. In fact, the 4 inch uniform factor may be anywhere between 0.0069 (pCi/g)/cps to 0.0133 (pCi/g)/cps. Factors for the 1inch and 2 inch Cs-137 distribution models are then calculated as a correction to the 4 inch base model. This leads to a total possible range for *K* from 0.0069 to 0.0333, accounting for all sources of uncertainty. Thus, the corresponding range in the size of the Cs-137 plume exceeding 17 pCi/g may be even greater than depicted in Figure 10.

The Cs-137 depth analysis presented in a previous section provides strong evidence for preference of the 1 inch or 2 inch models over the 4-inch model. Additional measurements or careful sampling may provide further basis for selecting a particular distribution model, thus eliminating a major uncertainty source. Laboratory measurements with the GPRS scintillator and development of a method for precisely defining the low-level discriminator can greatly reduce the second uncertainty source.

A final source of ambiguity arises from the choice of a background radiation level. Although the methods outlined for adopting an appropriate value are well supported, it is possible that background may range somewhat above or below 1300 cps. Figure 14 provides an illustration of the background effect on final concentration estimates. As in Figure 11, plotted outlines mark the limit of soil contamination exceeding 17 pCi/g. Differences between the boundary locations reflect changes in the assumed background from 1200 cps to 1400 cps. This analysis uses a *K* factor of .019 (pCi/g)/cps. Higher K factors produce greater movement of the contamination boundary, lower K factors produce lesser movement. Overall, the background effect is relatively small, with the greatest changes occurring along gentle concentration gradients. Conversely, virtually no change occurs over steep concentration gradients.

ARA-24 RESULTS

Processing and analysis of ARA-24 GPRS data followed the ARA-23 procedure. This section provides a succinct account of the major results at ARA-24. For greater discussion, see above.

Data Collection

Approximately 13,000 data points were collected by the GPRS system at ARA-24 following the same approach as described above for ARA-23 (Figure 15). Several gaps remain between the pre-defined survey boundary and the limit of data collection, particularly in the northeast portion of the site. However, the majority of ARA-24 shows little or no increase in radioactivity above background and the remaining data collection was suspended in favor of extending the ARA-23 survey. No Ge-spectrometer measurements were made at ARA-24.

Bulk gamma-ray fields and background analysis

Figure 16 shows a color intensity map depicting the bulk gamma radiation measured by the GPRS system at ARA-24. Soil contamination at ARA-24 is much less widespread and at lower concentrations than observed at ARA-23. Only the extreme southwest portion of the site exhibits any significant elevation in radiation levels. The vast majority of the site shows radiation levels at 1300 cps or less. The maximum count value recorded at ARA-24 was 14,645 cps, compared with 117,691 cps at ARA-23.

Background variation is highlighted in Figure 17. The central portion of the site formerly occupied by the ARA III facilities corresponds with slightly depressed background values (<1200 cps) compared with non-facility locations. The background depression is interpreted to result from human alterations of the shallow soil zone associated with facility operations and/or decontamination and decommissioning of ARA III. A background radiation level of 1250 cps was adopted by inspection of the non-facility portions of the ARA-24 survey data.

Conversion to activity concentration

The 1 inch uniform distribution model was used to convert the ARA-24 GPRS count data to estimates of Cs-137 activity concentration on the basis that this surficial distribution is appropriate for windblown deposition. Figure 18 presents results of this conversion. Note that contamination exceeding 17 pCi/g is confined to a small area (~ 1 acre) in the southwest portion of the site. The contamination area is bounded on all sides by steep concentration gradients, which indicates that the 17 pCi/g boundary will be relatively insensitive to uncertainties in the conversion factor or the adopted background level.

The contamination area begins about 100 - 150 feet southwest of the ARA-12 site, but the data indicate that the region between ARA-12 and the contamination area contains only slightly elevated (< 5 pCi/g) Cs-137. Due to inaccessible terrain, the GPRS survey terminated before reaching background radiation levels at the southwest terminus of the contamination area. Consequently the southwest limit of this contamination zone is currently undefined.

CONCLUSIONS AND RECOMMENDATIONS

The ARA-23 and ARA-24 in situ radiation surveys were successfully completed by the INEEL Environmental Monitoring GPRS system according to the adopted specifications. Over 69,000 independent measurements were collected at ARA-23 and over 13,000 were collected at ARA-24. These data were converted to estimates of in situ Cs-137 concentrations based on methods developed or adapted by INEEL radiation measurements personnel. Converted data were compiled into maps showing the quantitative distribution of Cs-137 across these sites. The following conclusions are offered:

1. Cs-137 concentration estimates computed based on scintillation detector data were quantitatively and qualitatively consistent with historical knowledge of the ARA site activities, with independently collected in situ Ge-spectrometer measurements, and with two

suites of sample results. Discrepancies between sample results and in situ concentration estimates, which occur primarily in areas of elevated radioactivity (>25 pCi/g), are most likely due to the difference in measurement scale between the two methods.

2. The precise Cs-137 concentration estimate at any given point was shown to depend on the assumed model for Cs-137 distribution with depth. A set of accessory Ge-spectrometer measurements focused on the Cs-137 K x-ray and the 662 keV gamma-ray clearly indicate that the Cs-137 contamination is present in the first 1 to 2 inches of soil. This information greatly reduces the uncertainty in concentration estimates, but is strictly applicable only in the vicinity of the accessory measurements.

3. Cs-137 concentration estimates are subject to additional uncertainty associated with detector's unknown low-level discriminator setting. This factor produces a +40% to -20% uncertainty in the Cs-137 concentration estimates, which may be reduced or eliminated by additional laboratory measurements.

4. Concentration estimates are somewhat sensitive to the choice of a background radiation level. Accessory data were collected to specifically evaluate background radiation levels so that the uncertainty range for background is estimated to be less than ± 100 cps. This cps range corresponds to a concentration range less than ± 1 - 2 pCi/g.

5. Final maps depicting Cs-137 concentration estimates for the ARA-23 and ARA-24 sites show the distribution and concentration of Cs-137 contamination in great detail. These maps permit unambiguous identification of highly contaminated zones, contaminated roadways, sharp and gradual contamination boundaries, satellite contamination zones, and clean areas.

6. At ARA-23, in situ Cs-137 concentration estimates show the contaminated area exceeding 17 pCi/g to include from 14.5 - 30.6 acres depending on the adopted Cs-137 distribution model. Data at ARA-24 show the contaminated area exceeding 17 pCi/g to include about 1 acre, regardless of the distribution model.

In addition, the following recommendations are offered:

1. Additional Ge-spectrometer measurements or focused soil sampling would be beneficial to characterizing the depth distribution of Cs-137 across the sites. Once an appropriate model for the depth distribution is adopted, the Cs-137 concentration estimates may be recalculated with considerably reduced uncertainty.

2. Laboratory measurements and calibration of the GPRS scintillation detector would minimize the uncertainty associated with the detector's low-level discriminator setting.

3. Additional soil sampling to ascertain the relative concentration and distribution of Sr-90 to Cs-137 across the ARA-23 and ARA-24 sites would be useful to determine if the Cs-137 data is a valid indicator for Sr-90 contamination.

FIGURES

ε : some, but not all photon-detector interactions produce a valid "count" depending on the detector efficiency

γ: photon energy affects photon attenuation and thus the number of "counts" recorded per disintegration

Ω: only photons traveling along a path contained within the sensor field of view will have a chance to interact with the detector

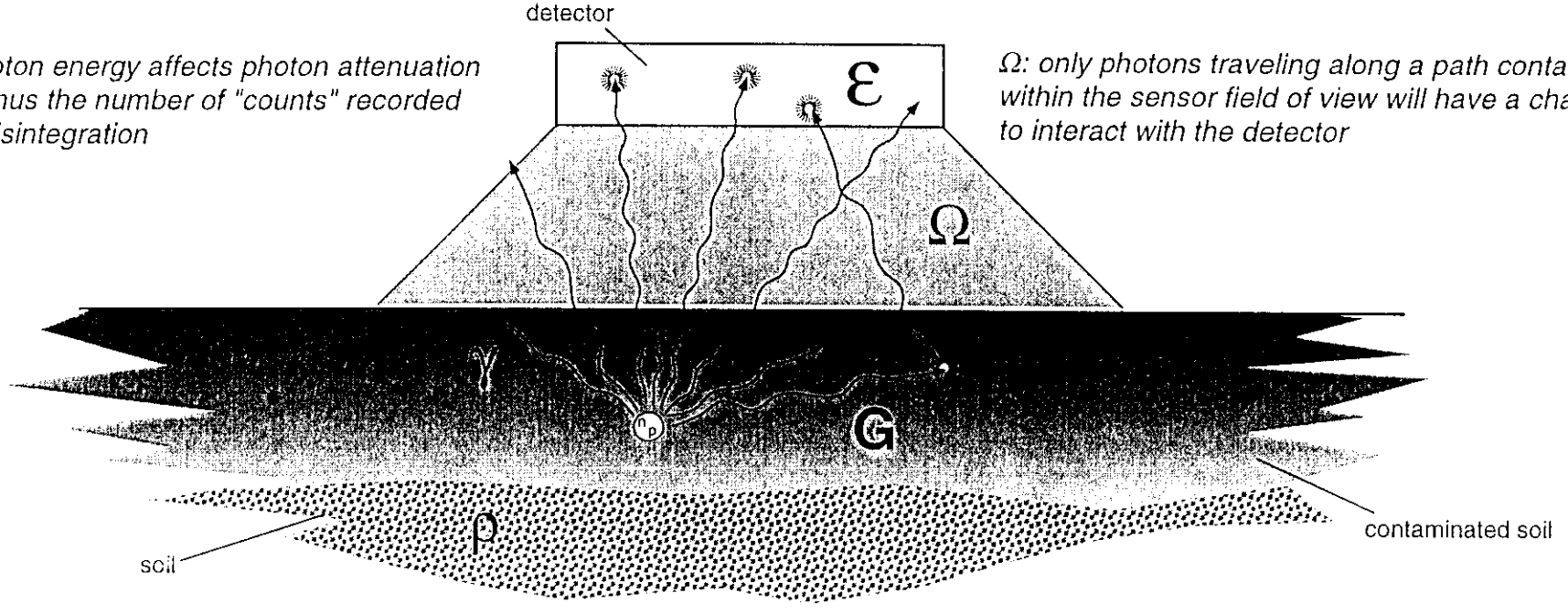

ρ: soil density affects photon attenuation and thus the number of "counts" recorded per disintegration

G: the source geometry (concentration and distribution) is the parameter solved for in the conversion process; normally distribution must be assumed in order to determine concnetration

FIGURE 1

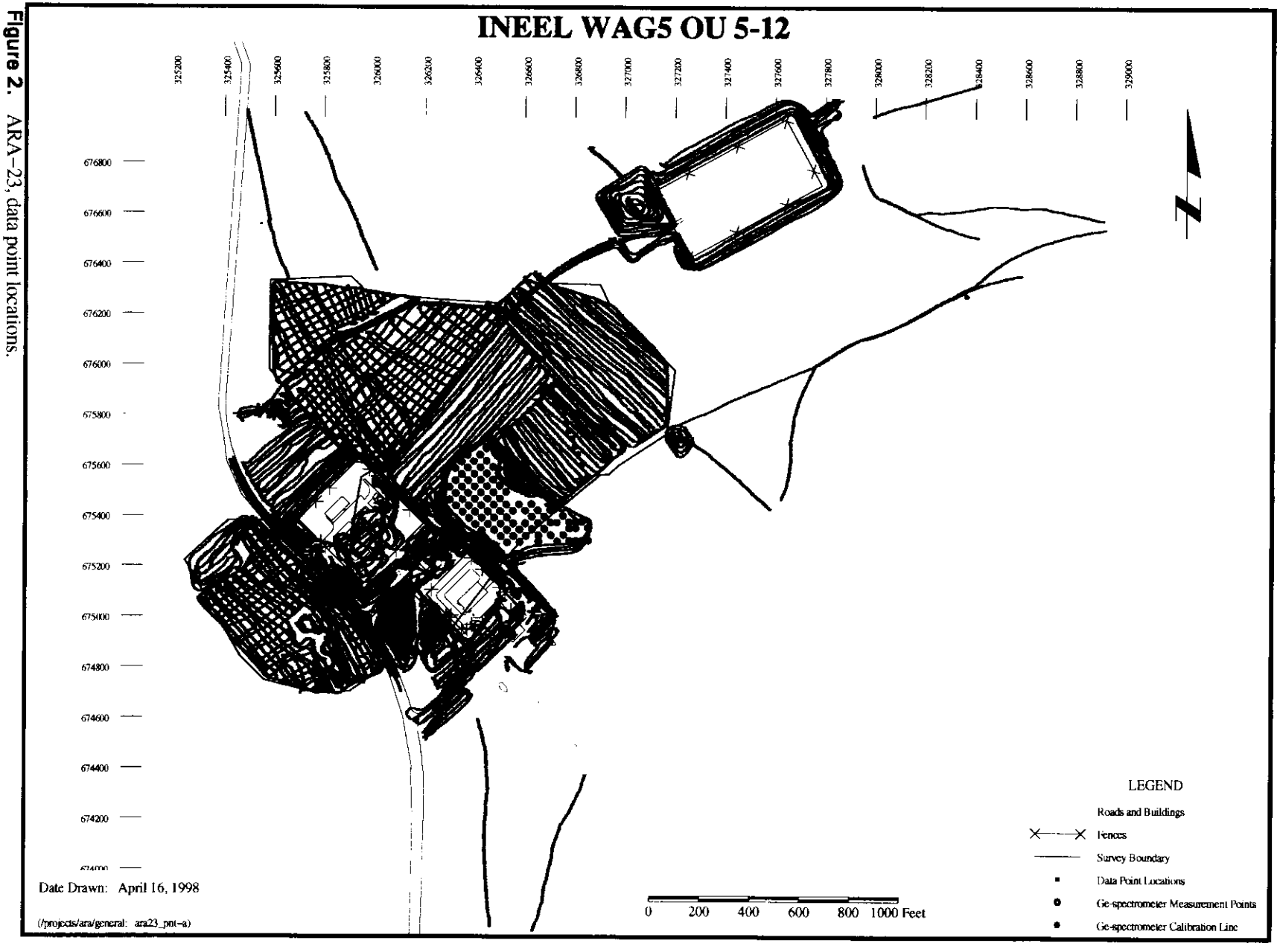

Figure 2. ARA–23, data point locations.

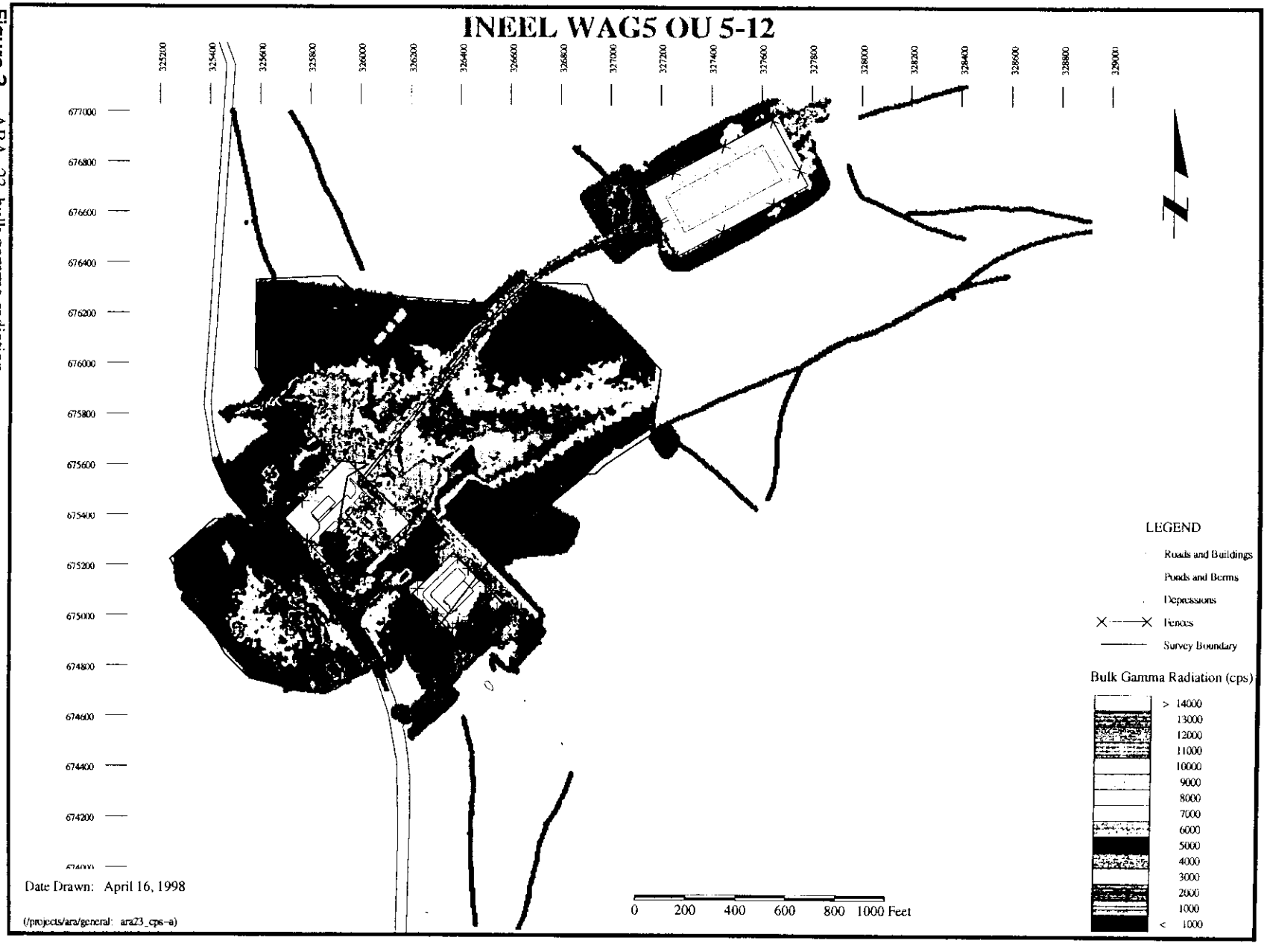

Figure 3. ARA-23, bulk gamma radiation.

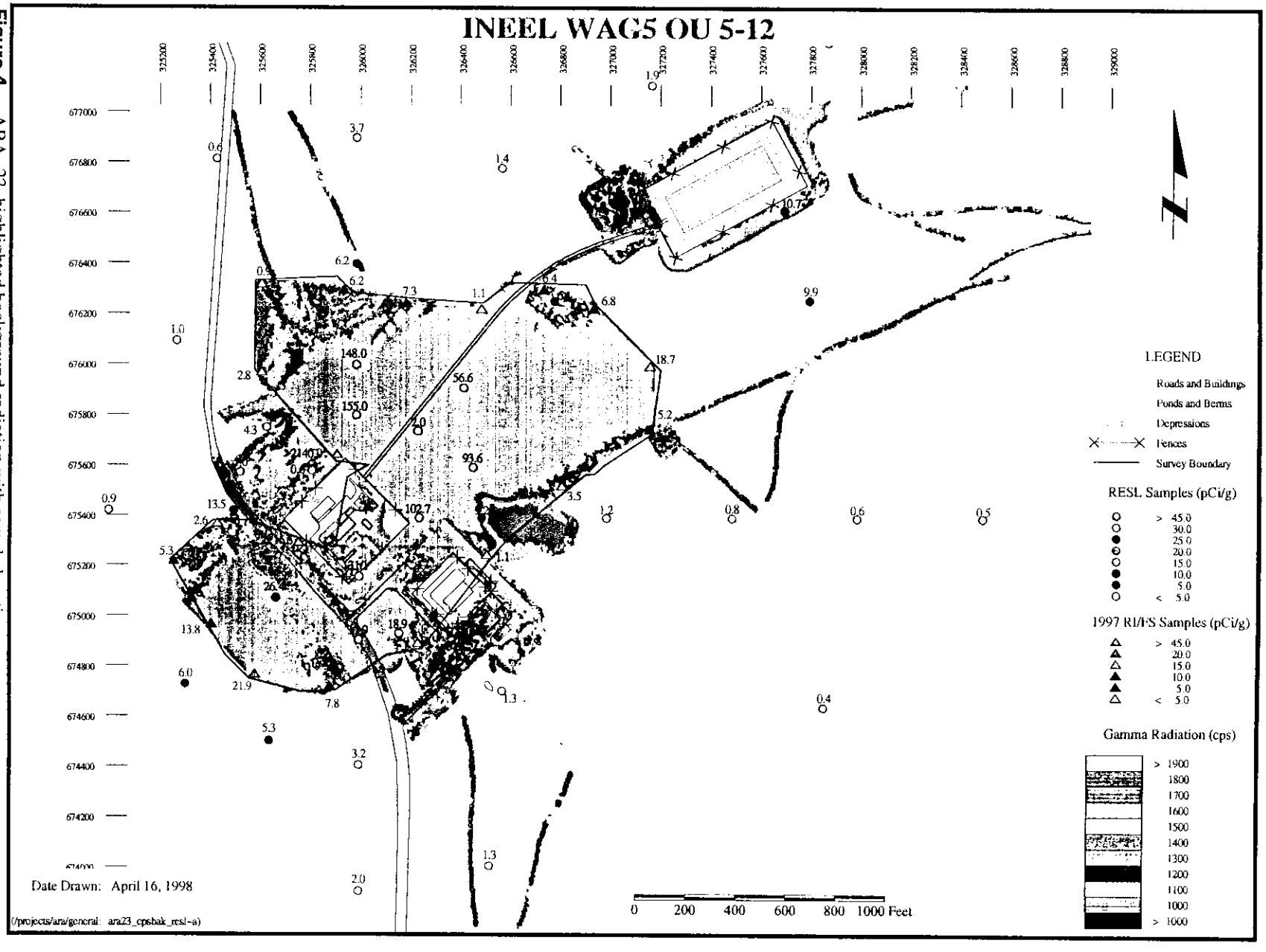

Figure 4. ARA–23, highlighted background radiation with sample locations.

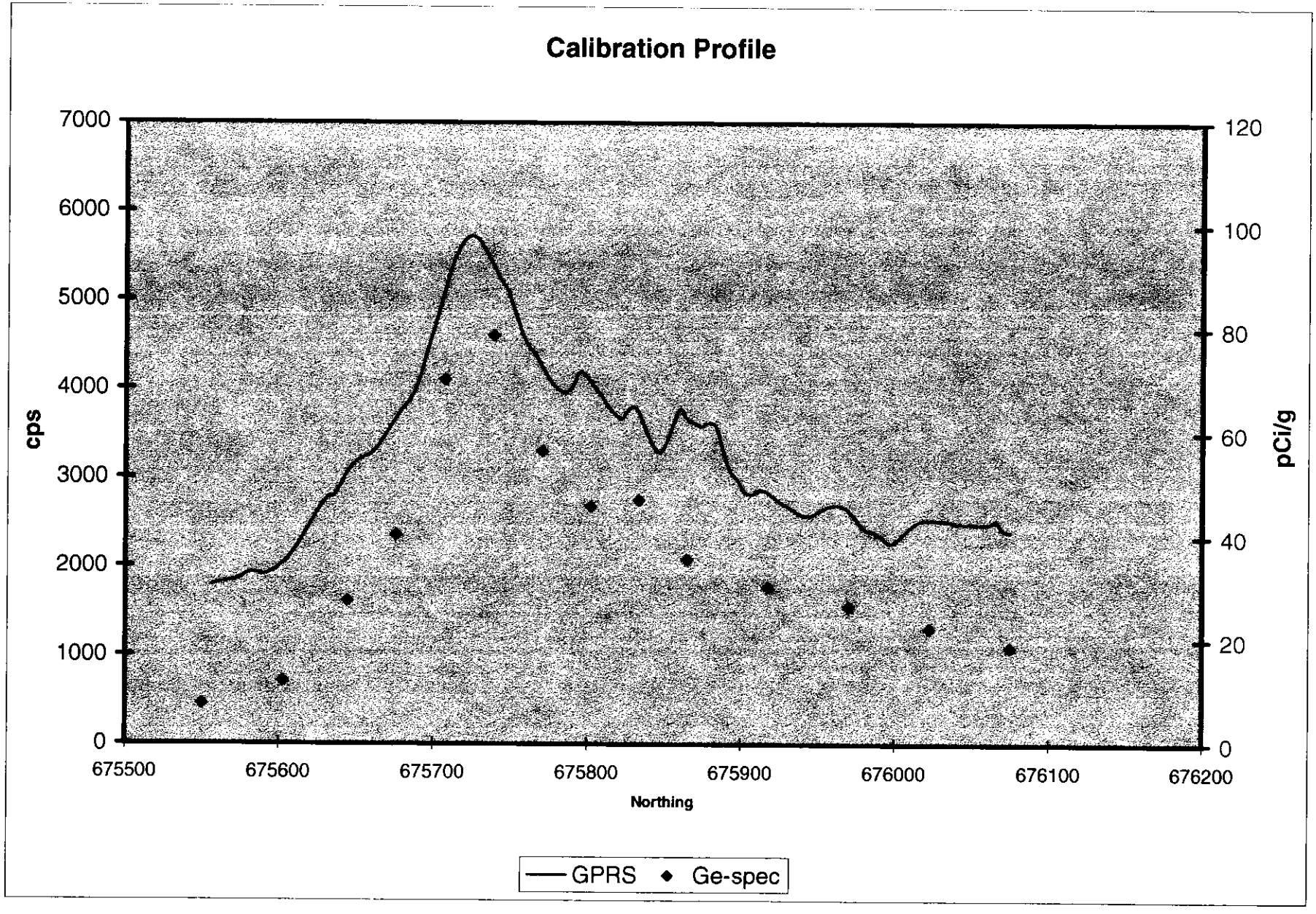
Calibration Profile
7000
6000
5000
4000
3000
2000
1000
0
cps
120
100
80
60
40
20
0
pCi/g
675500
675600
675700
675800
675900
676000
676100
676200
Northing
GPRS
Ge-spec

FIGURE 5

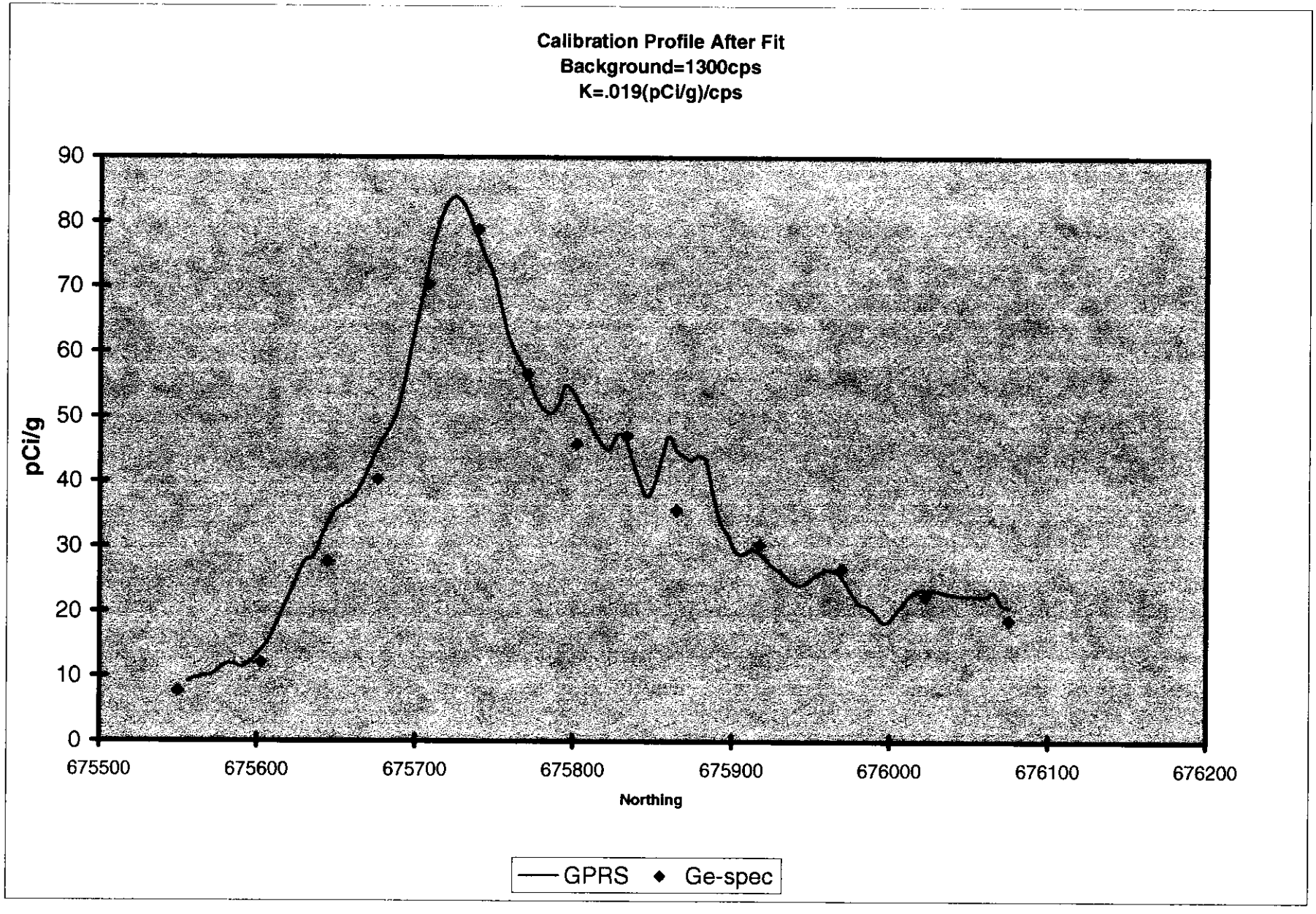
Calibration Profile After Fit
Background=1300cps
K=.019(pCi/g)/cps
pCi/g
90
80
70
60
50
40
30
20
10
0
675500
675600
675700
675800
675900
676000
676100
676200
Northing
GPRS
Ge-spec

FIGURE 6

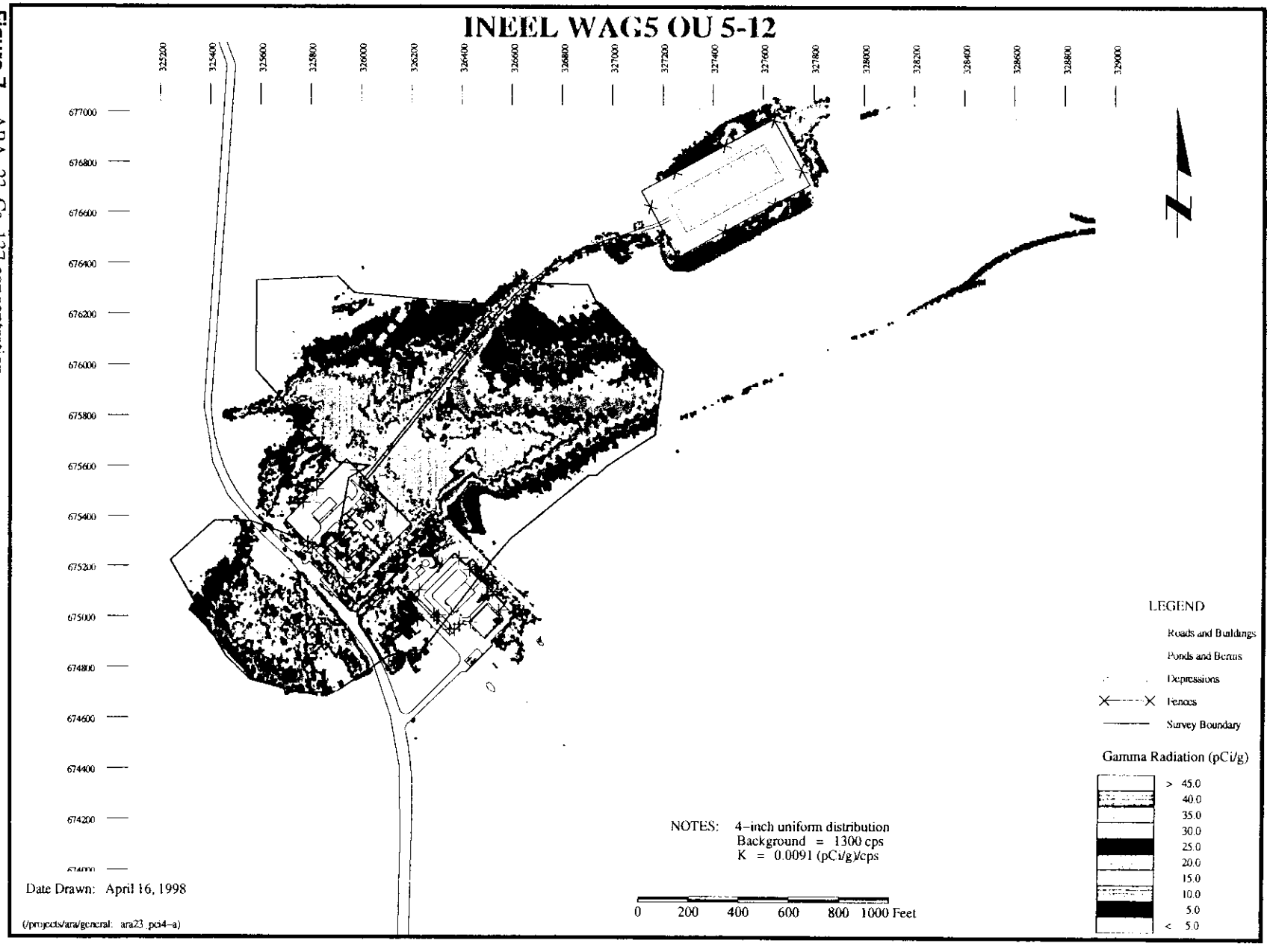

Figure 7. ARA-23, Cs-137 concentration.

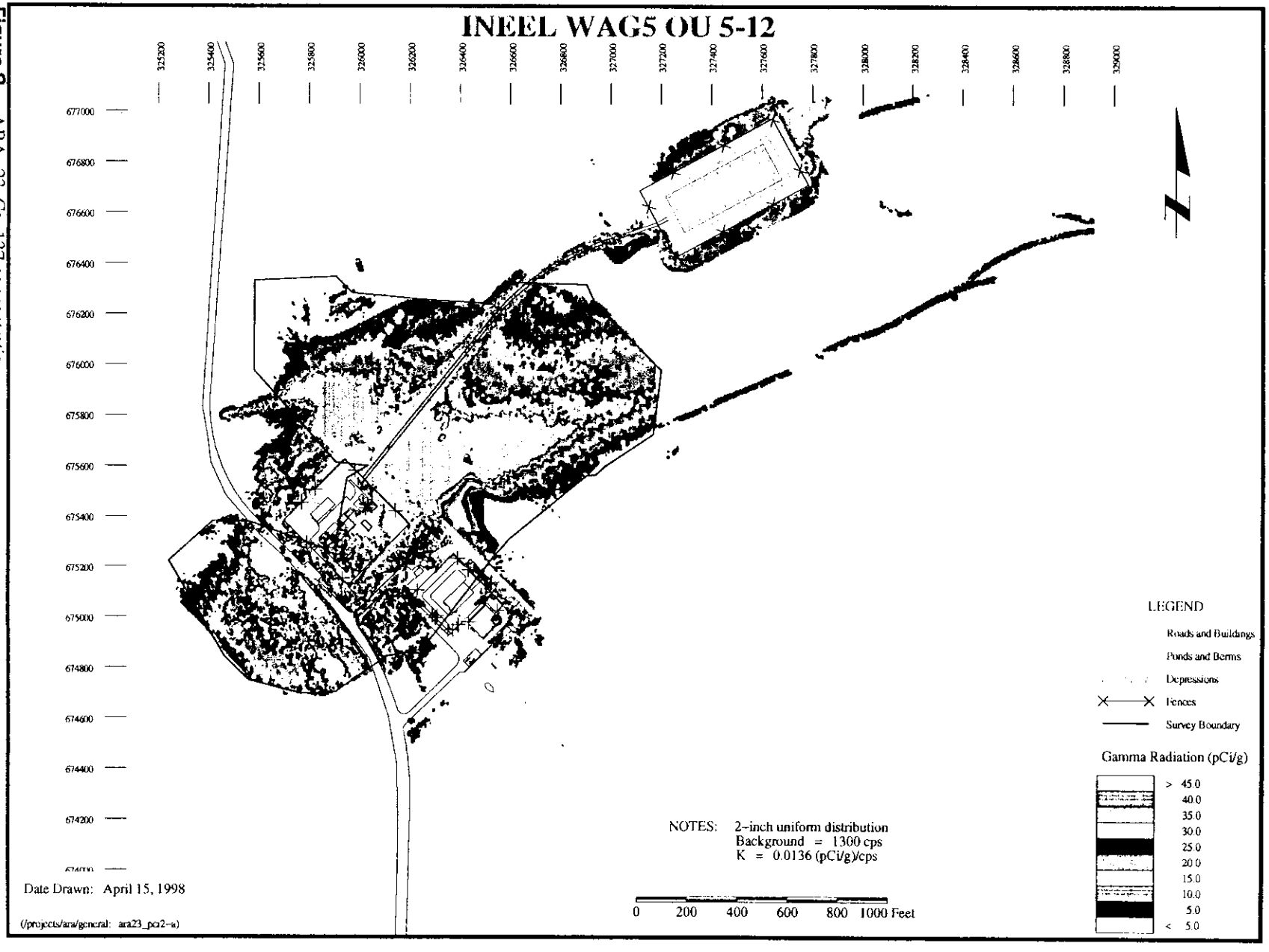

Figure 8. ARA-23, Cs-137 concentration.

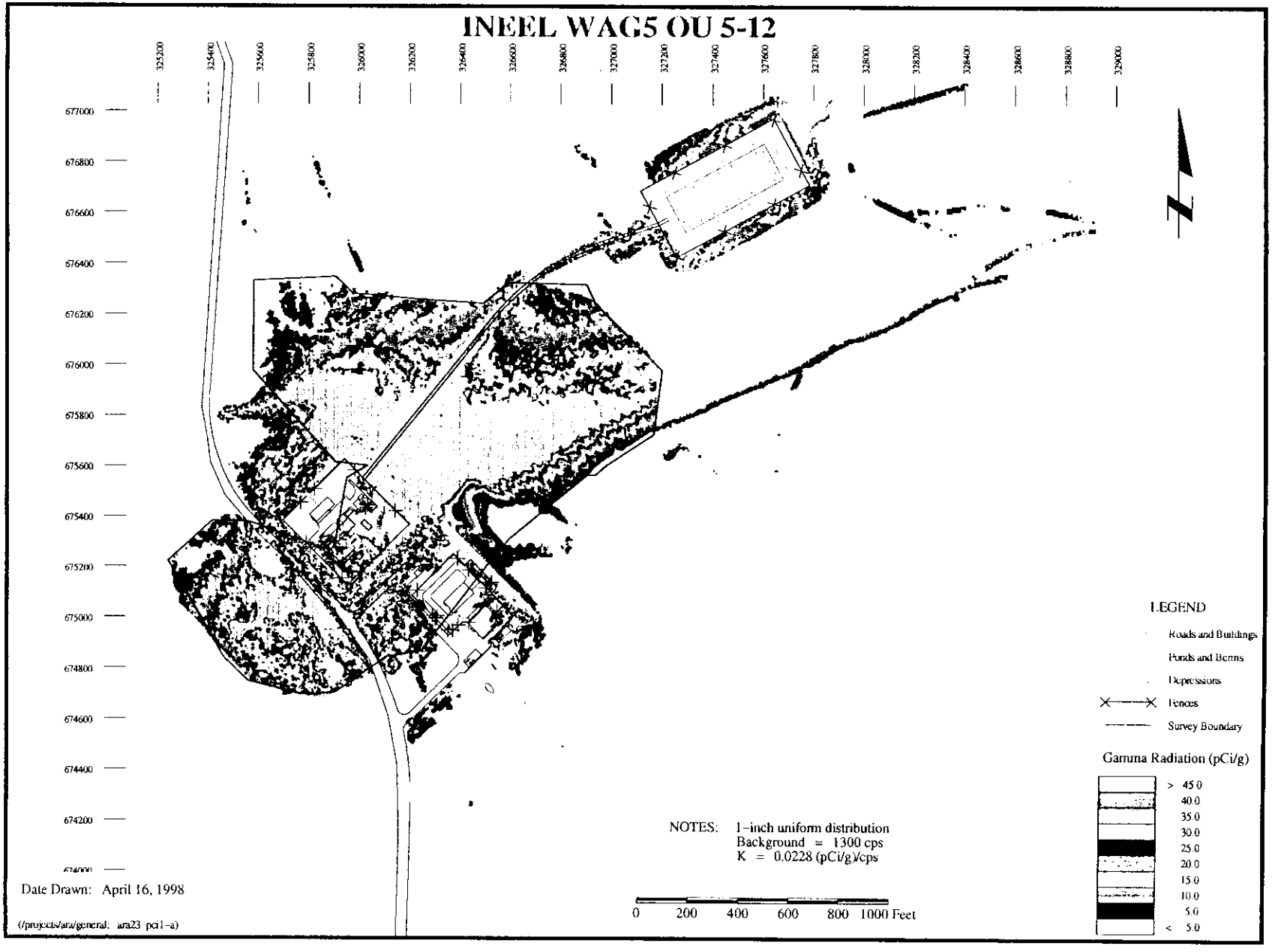

Figure 9. ARA-23, Cs-137 concentration.

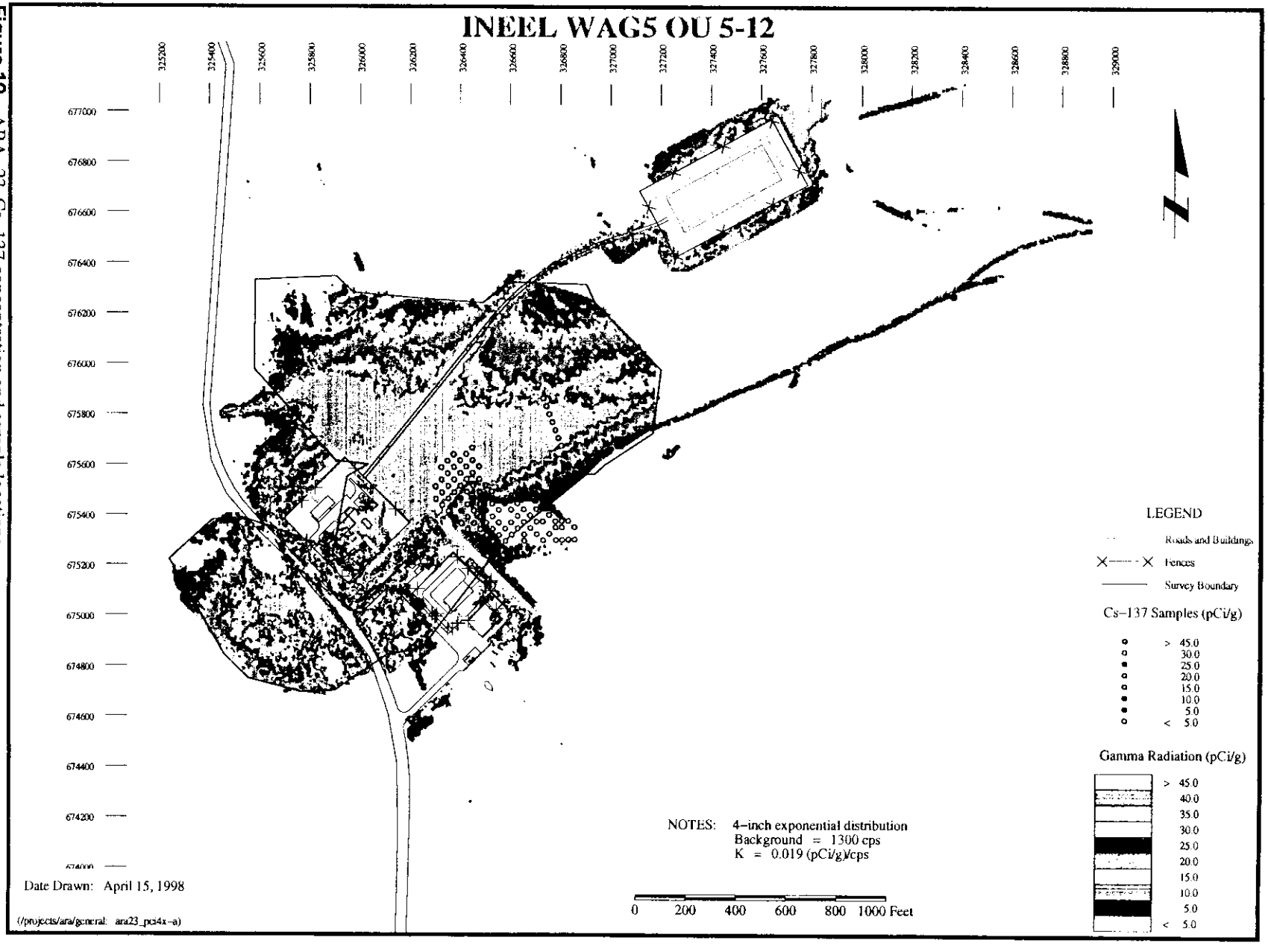

Figure 10. ARA-23, Cs-137 concentration and sample locations.

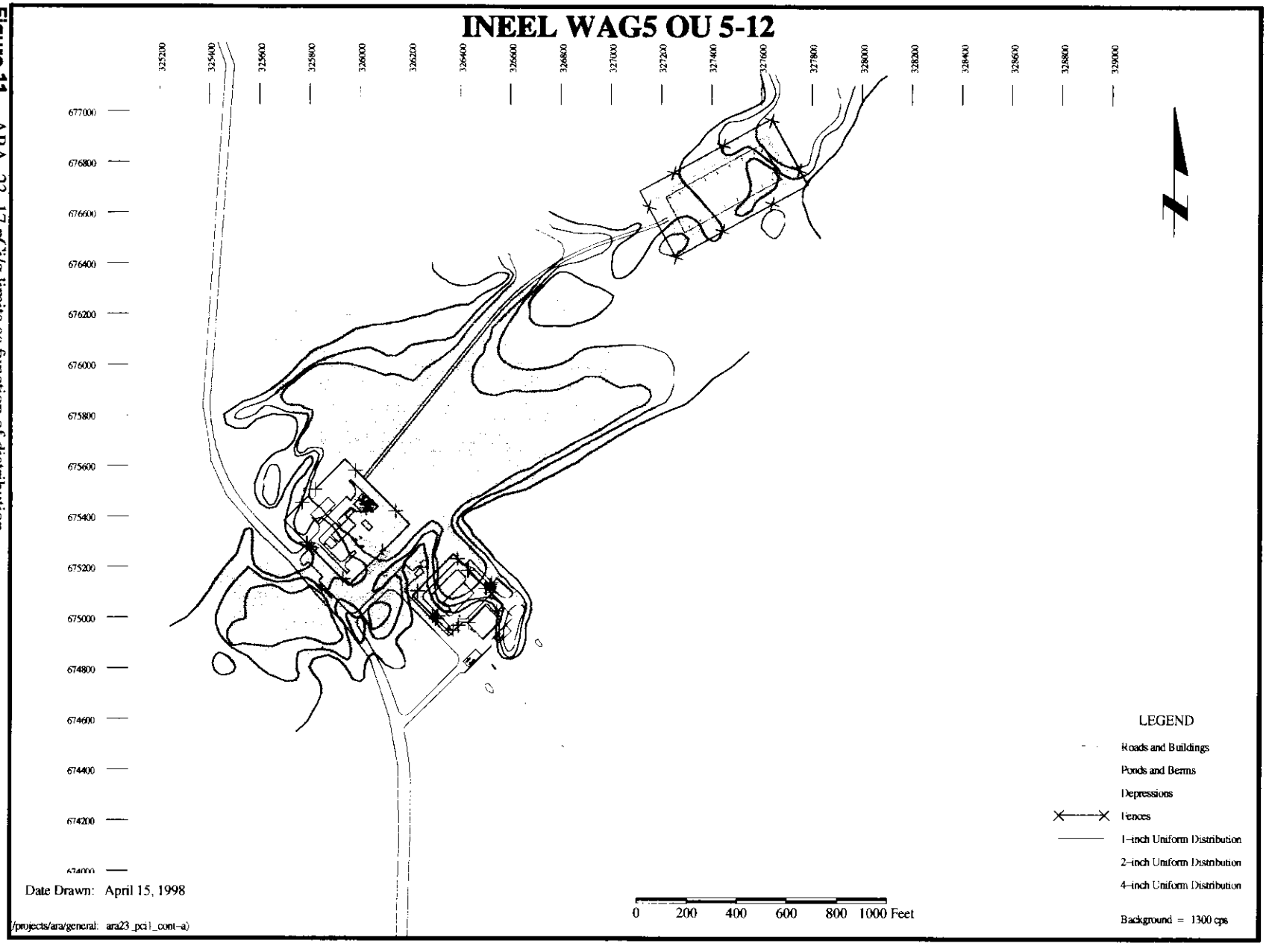

Figure 11. ARA-23, 17 pCi/g limits as function of distribution.

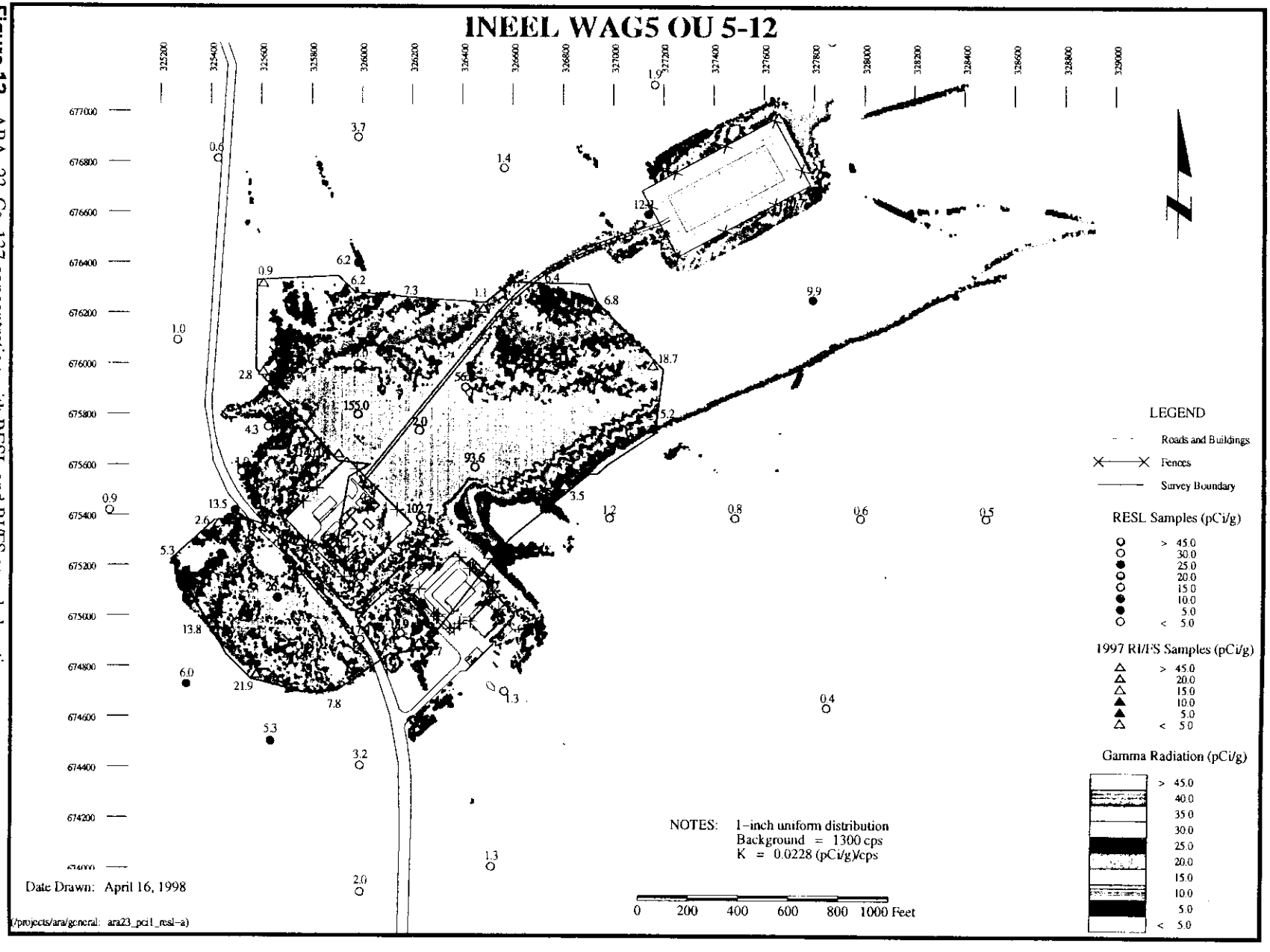

Figure 12. ARA-23, Cs-137 concentration with RESL and RI/FS sample locations.

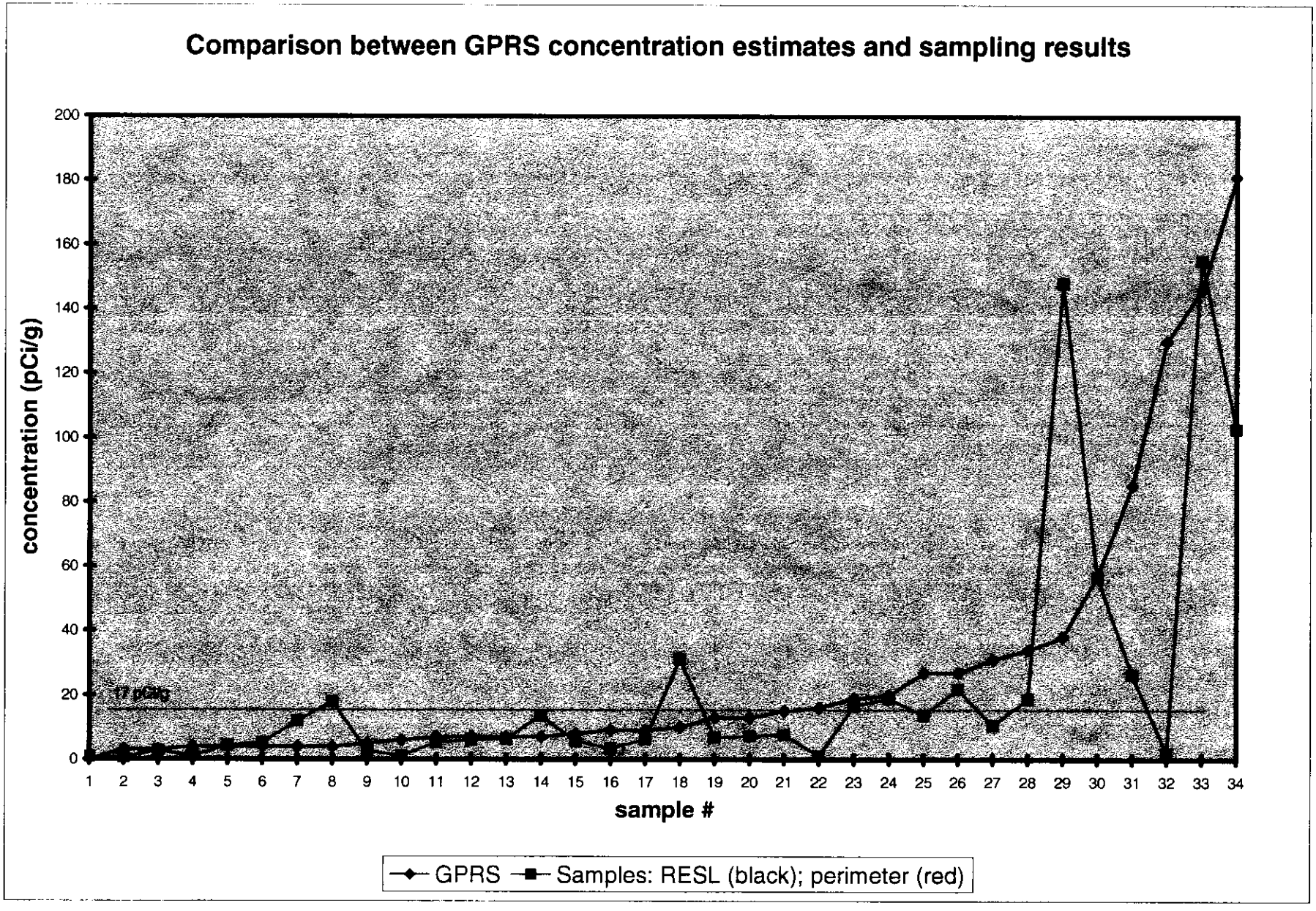
Comparison between GPRS concentration estimates and sampling results
concentration (pCi/g)
200
180
160
140
120
100
80
60
40
20
0
17 pCi/g
1 2 3 4 5 6 7 8 9 10 11 12 13 14 15 16 17 18 19 20 21 22 23 24 25 26 27 28 29 30 31 32 33 34
sample #
GPRS
Samples: RESL (black); perimeter (red)

FIGURE 13

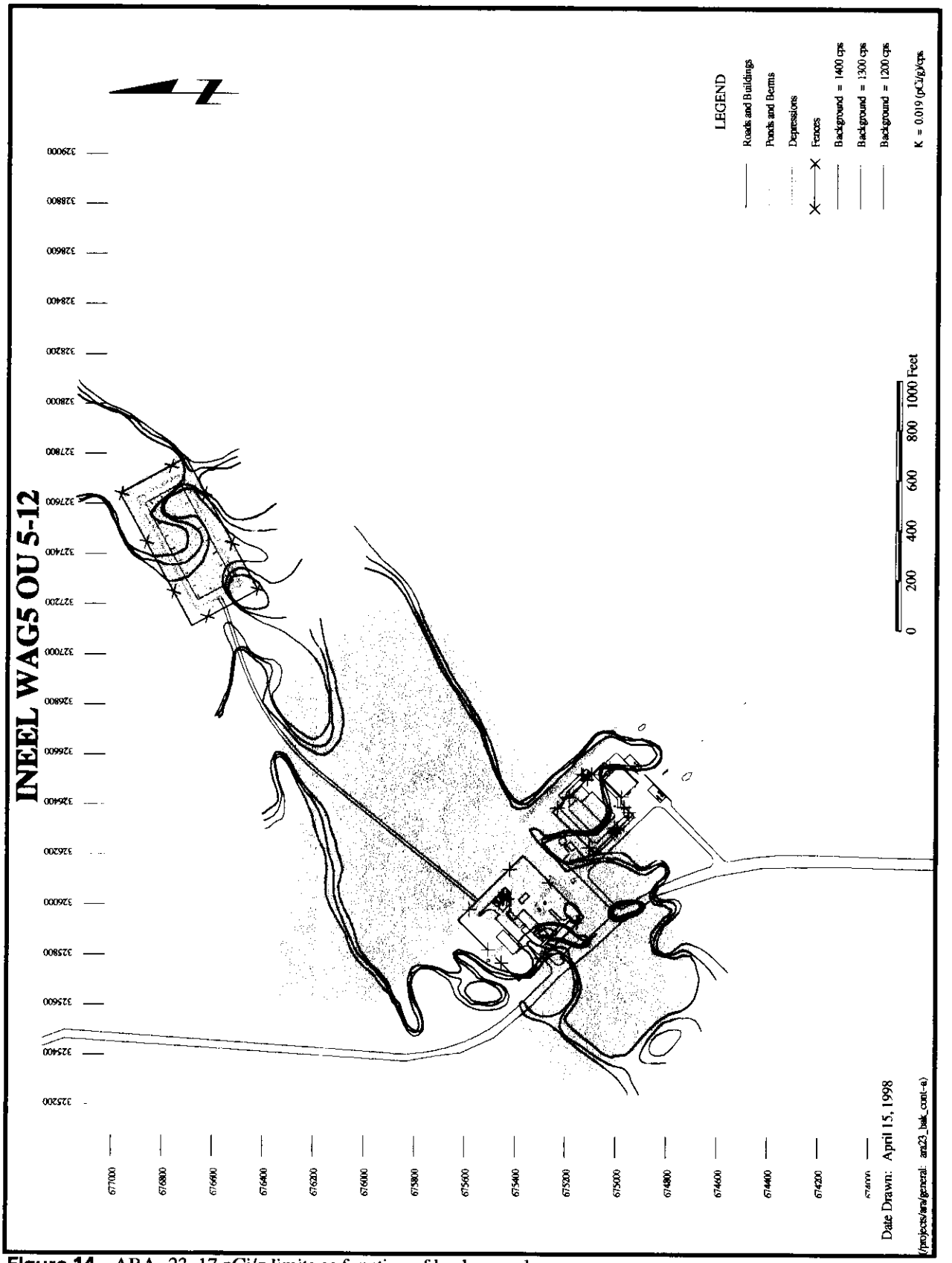

Figure 14. ARA–23, 17 pCi/g limits as function of background.

Figure 15. ARA–24, data point locations.

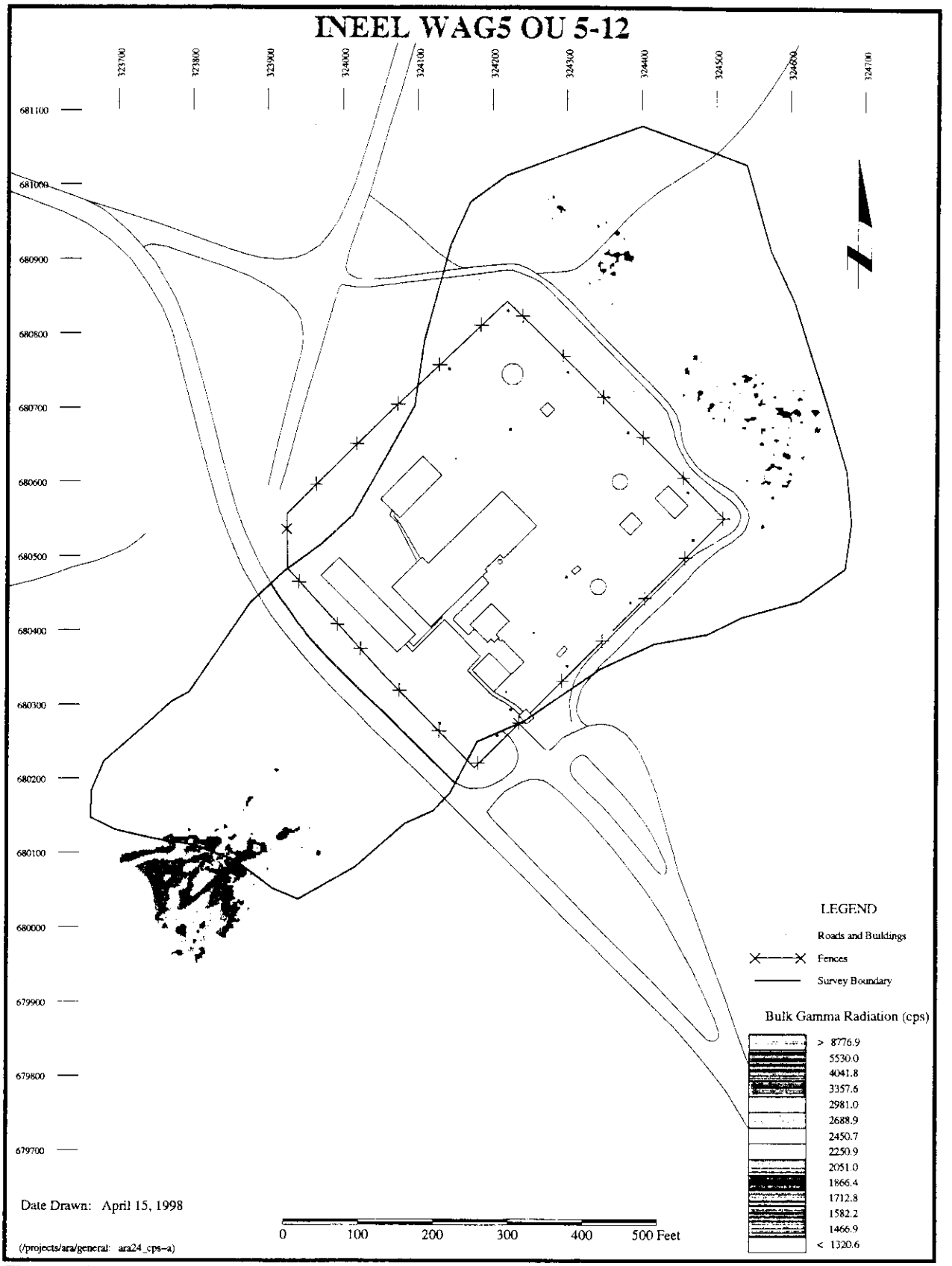

Figure 16. ARA–24, bulk gamma radiation.

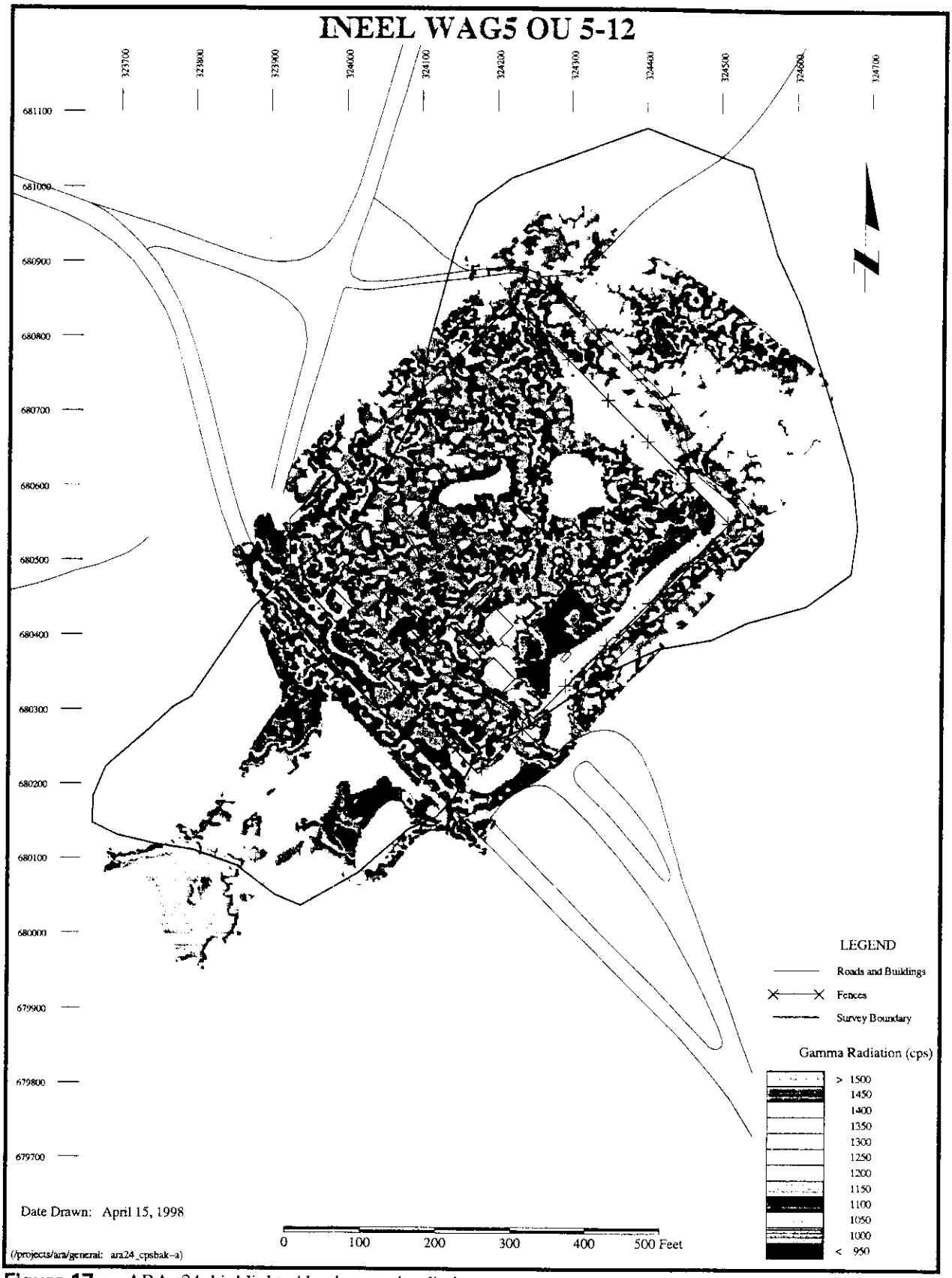

Figure 17. ARA–24, highlighted background radiation.

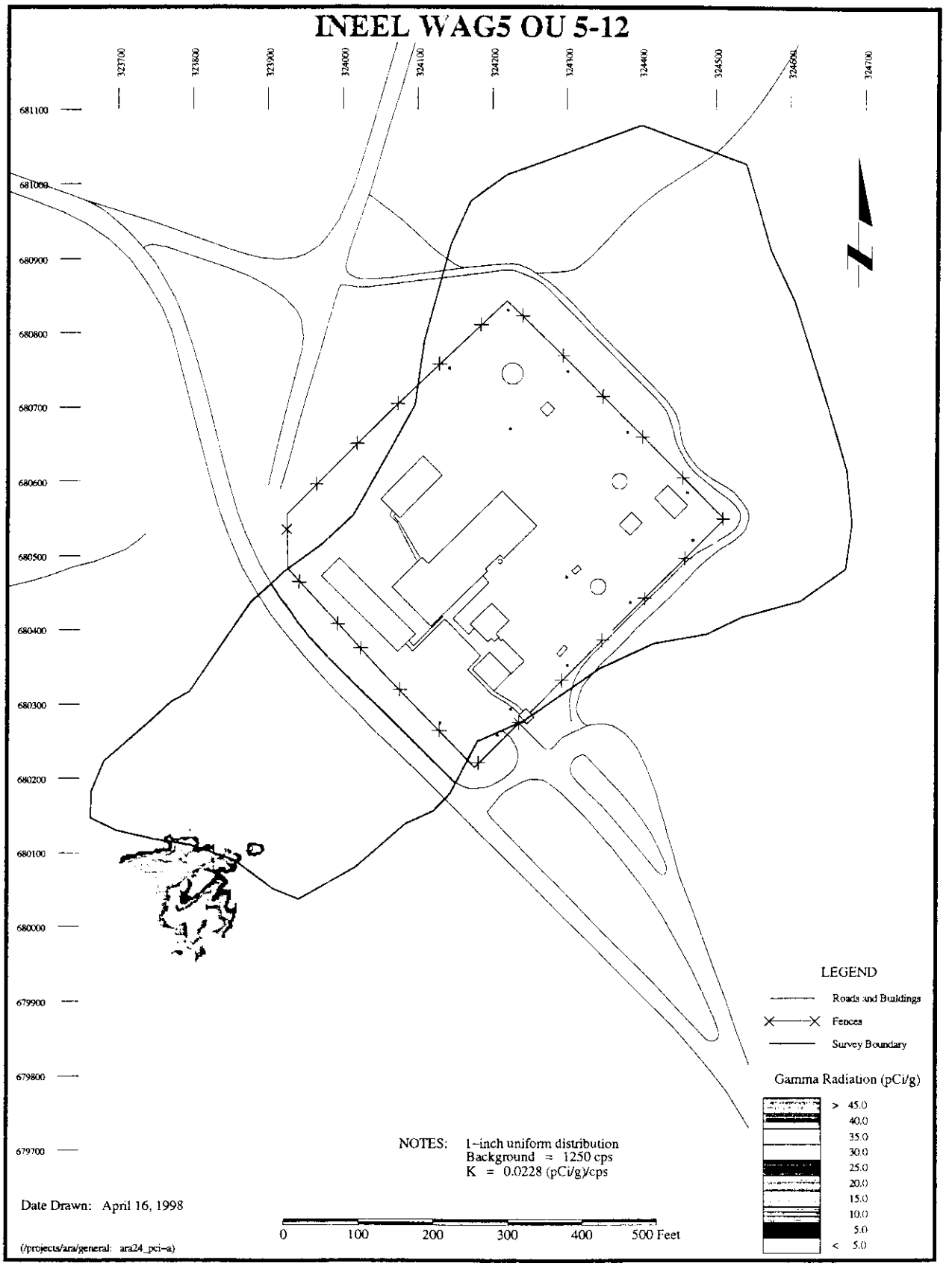

Figure 18. ARA–24, Cs–137 concentration.

ATTACHMENT 1

LOCKHEED MARTIN

Lockheed Martin Idaho Technologies Company

INTERDEPARTMENTAL COMMUNICATION

Date:	September 15, 1997		
To:	M. V. Carpenter	MS 2107	6-8467
From:	C.P. Oertel	MS 5202	6-3541
Subject:	RESULTS OF INSITU GAMMA RAY MEASUREMENTS AT ARA 23 - CPO-04-97		

We have completed insitu gamma ray analyses of 88 points located in the rockpile area of ARA 23. These measurements were performed using a 30% efficient p-type germanium detector held at a distance of one meter above ground. Each count duration was 600 seconds live time and all spectra were checked for gain stability in the field using the Cs-137 gamma ray at 661 kev and the K-40 gamma ray at 1460 kev. Spectra were analyzed using the USDOE Environmental Measurements Laboratory M1 protocol and software. Results are shown on the attached Excel spreadsheet.

The target isotope of interest for this work is Cs-137. During our recent meeting with Bob Gehrke and Dick Helmer, we agreed to assume a uniform distribution of Cs-137 with soil depth to four inches. In order to use M1 properly and report the Cs-137 values in pCi/g I assumed a relaxation length or depth (depth for the activity to decrease to 1/e) of four inches and a soil density of 1.6 g/cm^3. M1 uses the inverse of the relaxation length and the density in its calculations. The M1 protocol states that if a relaxation length of less than 4 inches is assumed, the software assumes a planar distribution and reports the Cs-137 in units of pCi/m^2. I mention this in the event that you are considering recalculation of the Cs-137 with different depth distributions. I can perform those calculations or I can calculate simple counts/sec for any of the spectra. It would also be interesting and useful to perform some measurements with an n-type extended energy range detector as suggested by Bob. This might allow inferences of the depth distributions which we currently do not have.

Finally, we are available to perform the additional background measurements suggested by Dick Helmer and yourself. Please contact me if you still want this work performed.

CPO/gjf

cc: R. J. Gehrke, MS 2114
R. L. Hand, MS 5210 (w/o Attach)
R. G. Helmer, MS 2114
C. M. Hiaring, MS 3953
K. L. Martin, MS 7113 (w/o Attach)
JW Rogers, MS 7113
F. L. Weber, MS 3953
R. N. Wilhelmsen, MS 4110
K. C. Wrighnt, MS 4110

ARA 23 RESULTS: Cs-137 (pCi/g) by location
α/ρ=0.059, ρ(soil)=1.6 g/cm^3
RELAXATION LENGTH= 4.2 INCHES

CPP RADIOCHEMISTRY GROUP 9/97
FIELD MEASUREMENTS: SJ HILL, BK HARRIS, KJ OLTMANNS, CP OERTEL
DATA ANALYSIS: CP OERTEL

Point ID	North	East	Elevation	Descriptor	Cs-137 (pCi/g)	Error (1σ)
43	675744.69	327157.65	5062.84	1409		
45	675519.6797	326807.6821	5048.781211	1820		
46	675244.701	326507.7292	5048.190371	2290		
50	675303.737	326856.3668	5044.37718	1009	2.27	0.07
51	675328.7173	326855.7158	5044.865007	1010		
52	675353.742	326855.0312	5045.785916	1011	2.28	0.07
53	675378.0687	326829.4661	5045.689839	1012	2.85	0.07
54	675352.9932	326829.9899	5046.732685	1013		
55	675328.0392	326830.7276	5045.46982	1014		
56	675303.0546	326831.3398	5044.429285	1015	2.96	0.07
57	675277.4055	326807.0023	5044.049412	1025		
58	675302.4133	326806.3045	5044.854863	1026	1.87	0.06
59	675327.4592	326805.7545	5044.596126	1027		
60	675352.6574	326805.3328	5047.931542	1028	1.37	0.06
61	675377.433	326804.4346	5046.556864	1029	3.43	0.08
62	675402.335	326803.7368	5046.002064	1030		
63	675401.6833	326778.7488	5045.907501	1031		
64	675376.6865	326779.3859	5047.490977	1032	1.82	0.06
65	675351.6612	326780.0584	5048.081828	1033	1.24	0.05
66	675326.7149	326780.7079	5045.259991	1034		
67	675301.5998	326781.3086	5043.727492	1035	1.59	0.06
68	675276.8133	326782.0105	5043.461811	1036		
69	675276.1472	326757.0416	5043.507705	1050		
70	675301.2179	326756.5073	5044.447654	1051		
71	675326.1296	326755.7322	5047.014996	1052	1.28	0.05
72	675351.1436	326755.1421	5045.622707	1053		
73	675376.0818	326754.3842	5047.966021	1054		
74	675401.1055	326753.8079	5046.313219	1055	1.86	0.06
75	675426.0899	326753.1818	5046.250684	1056		
76	675425.4559	326728.2734	5046.967459	1058		
77	675400.3911	326728.7804	5048.180975	1059		
78	675375.29	326729.2733	5048.090687	1060	1.66	0.06
79	675350.4003	326730.0992	5047.361644	1061		
80	675325.4817	326730.6747	5047.025283	1062		
81	675300.444	326731.3422	5045.428173	1063	1.56	0.06
82	675275.5435	326732.0383	5044.062974	1064		
83	675274.8408	326707.0309	5044.413949	1078		
84	675299.791	326706.392	5047.198912	1079		
85	675324.786	326705.6797	5046.4961	1080	1.32	0.05
86	675349.7831	326705.0688	5045.807912	1081		
87	675374.7714	326704.4601	5047.413038	1082	1.44	0.05
88	675399.7944	326703.7889	5048.652351	1083		
89	675424.7644	326703.136	5047.293443	1084	4.18	0.09

ARA 23 RESULTS: Cs-137 (pCi/g) by location
α/ρ=0.059, ρ(soil)=1.6 g/cm^3
RELAXATION LENGTH= 4.2 INCHES

CPP RADIOCHEMISTRY GROUP 9/97
FIELD MEASUREMENTS: SJ HILL, BK HARRIS, KJ OLTMANNS, CP OERTEL
DATA ANALYSIS: CP OERTEL

Point ID	North	East	Elevation	Descriptor	Cs-137 (pCi/g)	Error (1σ)
90	675449.0307	326677.3913	5049.183857	1088		
91	675424.0846	326678.1759	5049.85674	1089		
92	675399.073	326678.7622	5049.120606	1090	1.82	0.06
93	675374.0451	326679.4294	5047.847177	1091		
94	675349.2005	326680.0984	5048.022364	1092	1.16	0.05
95	675324.2016	326680.6934	5048.867026	1093		
96	675299.1723	326681.3733	5045.799852	1094		
97	675274.2148	326682.0154	5045.01986	1095		
98	675273.471	326656.9678	5045.449784	1105		
99	675298.5016	326656.3915	5047.65857	1106	2.03	0.06
10	,675323.47212589	,326655.75794233	,5048.0275415763	,1107.	1.22	0.05
10	,675348.53459248	,326655.14628146	,5049.2200849635	,1108.		
10	,675373.47510419	,326654.35838146	,5050.6363822356	,1109.	1.97	0.06
10	,675398.50202330	,326653.80678188	,5050.6556185105	,1110.		
10	,675423.45339175	,326653.12023734	,5050.2944122380	,1111.	2.66	0.07
10	,675448.46751783	,326652.45192801	,5049.5026743373	,1112.		
10	,675473.48193858	,326651.85261599	,5050.9206965857	,1113.		
10	,675472.77886238	,326626.85708505	,5051.2591544447	,1117.		
10	,675447.73515775	,326627.47793927	,5051.0436214496	,1118.	4.47	0.09
10	,675422.87444791	,326628.15573702	,5051.5531850309	,1119.		
11	,675397.90343688	,326628.78974187	,5050.0153111299	,1120.	2.15	0.06
11	,675372.87714152	,326629.47101010	,5048.8571386334	,1121.		
11	,675347.90326831	,326630.10398013	,5047.7589065021	,1122.	0.93	0.04
11	,675322.92347636	,326630.83766795	,5049.9855441914	,1123.		
11	,675297.91337941	,326631.40954894	,5048.9303300981	,1124.		
11	,675272.95778094	,326632.16541610	,5046.1923707427	,1125.		
11	,675272.34511423	,326607.15215687	,5046.5921586133	,1133.		
11	,675297.30964278	,326606.39659851	,5048.8285225107	,1134.		
11	,675322.18879097	,326605.78004788	,5049.7116179093	,1135.	3.12	0.08
12	,675347.22814336	,326605.14524807	,5050.0668325708	,1136.		
12	,675371.68665247	,326603.56962285	,5048.5855042052	,1137.	1.63	0.06
12	,675397.20406023	,326603.79886400	,5050.3023454455	,1138.		
12	,675422.15669481	,326603.11218779	,5052.0045905713	,1139.	2.55	0.07
12	,675447.18797548	,326602.56144211	,5051.5661022571	,1140.		
12	,675472.20082170	,326601.89770834	,5051.2519281951	,1141.		
12	,675497.17137283	,326601.19346286	,5052.3008951477	,1142.		
12	,675496.47252609	,326576.23094119	,5053.1431419916	,1146.		
12	,675471.58561460	,326576.84851385	,5049.8369680293	,1147.		
12	,675446.63172663	,326577.66340020	,5051.5657956913	,1148.	6..00	0.01
13	,675421.59231015	,326578.18320251	,5049.1269360859	,1149.		
13	,675396.60894411	,326578.90902814	,5048.7446196667	,1150.		
13	,675371.63527903	,326579.57000695	,5049.5156071210	,1151.		
13	,675346.61972258	,326580.13238115	,5049.5523302528	,1152.	1.77	0.06

ARA 23 RESULTS: Cs-137 (pCi/g) by location
α/ρ=0.059, ρ(soil)=1.6 g/cm^3
RELAXATION LENGTH= 4.2 INCHES

CPP RADIOCHEMISTRY GROUP 9/97
FIELD MEASUREMENTS: SJ HILL, BK HARRIS, KJ OLTMANNS, CP OERTEL
DATA ANALYSIS: CP OERTEL

Point ID	North	East	Elevation	Descriptor	Cs-137 (pCi/g)	Error (1s)
13	,675321.63372270	,326580.84183304	,5049.8340339905	,1153.		
13	,675296.62330215	,326581.43951789	,5049.8402083335	,1154.	4.14	0.09
13	,675271.61848025	,326582.12836207	,5047.6585568295	,1155.		
13	,675246.61643507	,326582.70691054	,5047.1908316699	,1156.		
13	,675246.07646141	,326557.80494055	,5047.9580207926	,1160.		
13	,675270.97976385	,326557.05527701	,5049.3755515124	,1161.		
14	,675296.00558985	,326556.40141633	,5050.6074057213	,1162.		
14	,675320.98827505	,326555.78756336	,5050.1481783853	,1163.	3.41	0.08
14	,675345.99931226	,326555.09939887	,5050.7680006257	,1164.		
14	,675370.92053093	,326554.52473262	,5050.8446166507	,1165.	2.18	0.06
14	,675395.88762587	,326553.76224502	,5050.4867238120	,1166.		
14	,675420.88876175	,326553.18196011	,5052.2274785188	,1167.	4.23	0.09
14	,675445.91972943	,326552.65840301	,5052.8885763742	,1168.		
14	,675470.90247546	,326551.89284400	,5051.5464924017	,1169.		
14	,675495.89599596	,326551.26599521	,5052.3343082597	,1170.		
14	,675520.91249350	,326550.63810614	,5053.1156155327	,1172.		
15	,675245.34623456	,326532.77419368	,5048.2508685579	,1186.		
15	,675270.35892566	,326532.19749167	,5049.1548213734	,1187.		
15	,675295.33228990	,326531.44671922	,5050.4865643351	,1186.	14.01	0.15
15	,675320.30872510	,326530.82665972	,5050.8066348444	,1185.		
15	,675345.25133216	,326530.12319122	,5051.7461460707	,1184.	4.65	0.09
15	,675370.34548998	,326529.57977657	,5051.3278820931	,1183.		
15	,675395.29106350	,326528.86807924	,5049.5264841783	,1182.	2.82	0.07
15	,675420.30579114	,326528.20755352	,5052.7183528769	,1181.		
15	,675445.26284227	,326527.54937198	,5053.2310615335	,1180.	3.83	0.08
15	,675470.27486111	,326526.81385109	,5053.9428345368	,1179.		
16	,675495.27709692	,326526.23137849	,5052.7748579446	,1178.	19.50	0.20
16	,675520.31042662	,326525.71669270	,5053.4744370173	,1177.		
16	,675544.58345778	,326499.94913309	,5053.0607094143	,1200.		
16	,675519.61914621	,326500.74562787	,5055.5377074817	,1199.	24.60	0.21
16	,675494.60988733	,326501.29891445	,5054.7725207284	,1198.		
16	,675469.58900360	,326501.88378439	,5054.3674159370	,1197.	7.45	0.11
16	,675444.61853281	,326502.64389387	,5052.4940224265	,1196.		
16	,675419.61362456	,326503.20749081	,5051.7180282868	,1195.	5.09	0.09
16	,675394.65698630	,326503.84818135	,5051.7196225451	,1194.		
17	,675369.71039663	,326504.51487917	,5052.3748674916	,1193.	4.89	0.09
17	,675344.71662578	,326505.23186074	,5053.8277912446	,1192.		
17	,675319.71841619	,326505.84172477	,5052.9764276946	,1191.	12.20	0.14
17	,675294.68102057	,326506.36596596	,5050.7318652955	,1190.		
17	,675269.68342645	,326507.12018647	,5048.3040555563	,1189.		
17	,675568.99983322	,326474.32904206	,5054.6663105595	,1205.		
17	,675618.91105021	,326473.10121727	,5055.0140217950	,1203.		
17	,675593.89878745	,326473.79700912	,5055.6303279355	,1204.	86.80	0.40

ARA 23 RESULTS: Cs-137 (pCi/g) by location
α/ρ=0.059, ρ(soil)=1.6 g/cm³
RELAXATION LENGTH= 4.2 INCHES

CPP RADIOCHEMISTRY GROUP 9/97
FIELD MEASUREMENTS: SJ HILL, BK HARRIS, KJ OLTMANNS, CP OERTEL
DATA ANALYSIS: CP OERTEL

Point ID	North	East	Elevation	Descriptor	Cs-137 (pCi/g)	Error (1s)
17	,675594.60036231	,326498.74853153	,5053.6550141410	,1202.		
17	,675544.00662600	,326475.01825319	,5055.1662147778	,1206.	50.90	0.29
18	,675519.00415936	,326475.68162081	,5055.0288325951	,1207.		
18	,675493.98517873	,326476.23954341	,5055.3161727796	,1208.	14.10	0.15
18	,675469.02335489	,326477.07677516	,5055.3797125580	,1209.		
18	,675443.98815825	,326477.58038793	,5054.7784476422	,1210.	12.60	0.15
18	,675419.03013131	,326478.22661386	,5052.6928616559	,1211.		
18	,675393.96280503	,326478.85950446	,5053.0179955476	,1212.	12.20	0.14
18	,675369.01337724	,326479.59550284	,5053.9237771720	,1213.		
18	,675344.07374974	,326480.32909523	,5054.2243248823	,1214.	17.50	0.17
18	,675318.94744429	,326480.70996594	,5050.8779969670	,1215.		
18	,675294.04743241	,326481.55499547	,5048.5930883808	,1216.		
19	,675318.38685407	,326455.80344187	,5049.5455857091	,1219.		
19	,675343.40596143	,326455.22787228	,5054.0145666783	,1220.		
19	,675368.39529640	,326454.53275452	,5053.7773799700	,1221.	21.60	0.19
19	,675393.42913731	,326453.94425445	,5054.1716232773	,1222.		
19	,675418.38429987	,326453.28685597	,5053.5548731636	,1223.	15.40	0.16
19	,675443.39536111	,326452.59209773	,5051.6134947024	,1224.		
19	,675468.30372916	,326452.05423004	,5056.2671548079	,1225.	14.40	0.16
19	,675493.26610863	,326451.20777797	,5055.1974158686	,1226.		
19	,675518.30382510	,326450.66662723	,5056.7615616255	,1227.	22.50	0.20
19	,675543.31161637	,326450.05727605	,5057.6087019945	,1228.		
20	,675568.29998159	,326449.33760071	,5057.8241522162	,1229.	67.20	0.36
20	,675593.30084791	,326448.80232623	,5055.9620399948	,1230.		
20	,675618.33084896	,326448.22875366	,5058.2789387630	,1231.	74.40	0.38
20	,675643.29303804	,326447.58854016	,5058.1251354899	,1232.		
20	,675642.60841113	,326422.54993456	,5059.2616816495	,1233.	64.60	0.35
20	,675617.67850251	,326423.09449619	,5059.6913156411	,1234.		
20	,675592.70239779	,326423.83050955	,5057.5335970441	,1235.	95.60	0.43
20	,675567.67310802	,326424.48930063	,5056.5831517012	,1236.		
20	,675542.69878261	,326425.08783679	,5055.9016647451	,1237.	41.60	0.30
20	,675517.74592541	,326425.79373831	,5056.1457655478	,1238.		
21	,675492.69950259	,326426.28702995	,5053.4042946175	,1239.	18.30	0.18
21	,675467.72327007	,326426.93477985	,5055.2763983651	,1240.		
21	,675442.67393367	,326427.54221181	,5055.2197331073	,1241.	21.30	0.19
21	,675417.71158398	,326428.33597626	,5054.8200323596	,1242.		
21	,675392.68336629	,326428.87335493	,5054.7897642367	,1243.	24.10	0.20
21	,675367.74565776	,326429.60560360	,5054.3846562609	,1244.		
21	,675342.74281604	,326430.29530399	,5052.1606532526	,1245.	33.70	0.24
21	,675342.11497728	,326405.24346882	,5051.6360608757	,1248.		
21	,675367.14554007	,326404.64711269	,5055.1291033242	,1249.	31.70	0.23
22	,675392.11492216	,326403.91884481	,5056.0086755696	,1250.		
22	,675417.13452692	,326403.39427871	,5054.9281250883	,1251.	29.50	0.22

ARA 23 RESULTS: Cs-137 (pCi/g) by location
α/ρ=0.059, ρ(soil)=1.6 g/cm^3
RELAXATION LENGTH= 4.2 INCHES

CPP RADIOCHEMISTRY GROUP 9/97
FIELD MEASUREMENTS: SJ HILL, BK HARRIS, KJ OLTMANNS, CP OERTEL
DATA ANALYSIS: CP OERTEL

Point ID	North	East	Elevation	Descriptor	Cs-137 (pCi/g)	Error (1s)
22	,675442.09325536	,326402.62896610	,5055.1558321353	,1252.		
22	,675467.12558160	,326402.08651787	,5055.2946224680	,1253.	26.70	0.21
22	,675492.13183967	,326401.42357265	,5053.9546957149	,1254.		
22	,675517.00252964	,326400.63709176	,5054.9602862377	,1255.	49.20	0.25
22	,675541.96928978	,326400.12112875	,5056.5377964545	,1256.		
22	,675567.02300528	,326399.50687471	,5056.8685589152	,1257.	119.00	0.50
22	,675592.01684913	,326398.80834694	,5058.7824372220	,1258.		
22	,675617.00982224	,326398.10495169	,5057.4461315254	,1259.	84.50	0.40
23	,675591.40436548	,326373.77257408	,5057.8325782203	,1260.	95.20	0.40
23	,675566.41070206	,326374.40641982	,5058.0192223955	,1261.		
23	,675541.40871678	,326375.14501733	,5055.8006802743	,1262.	102.00	0.40
23	,675516.40641895	,326375.76213354	,5055.9893627334	,1263.		
23	,675490.79071226	,326375.52185369	,5054.6820617258	,1264.	49.10	0.29
23	,675466.40545696	,326377.07011996	,5054.9145750105	,1265.		
23	,675441.42737328	,326377.65533927	,5054.5550894568	,1266.	28.10	0.22
23	,675416.42176822	,326378.39001580	,5054.6417569213	,1267.		
23	,675391.37365580	,326378.83321827	,5056.0073108143	,1268.	29.10	0.22
23	,675366.50480269	,326379.62281346	,5055.0088901969	,1269.		
24	,675341.49533642	,326380.18860317	,5052.2419355181	,1270.		
24	,675365.80721231	,326354.60005376	,5053.6382503551	,1271.		
24	,675390.82037642	,326353.94185751	,5054.7073986156	,1272.		
24	,675415.78133181	,326353.24754456	,5055.5178795442	,1273.	31.10	0.23
24	,675440.78588142	,326352.53156681	,5054.0587489628	,1274.		
24	,675465.83731883	,326352.13212351	,5054.3585791678	,1275.	50.40	0.30
24	,675490.79216100	,326351.35841186	,5056.0891045871	,1276.		
24	,675515.81633123	,326350.94297300	,5057.6630526217	,1277.	88.70	0.38
24	,675540.78623740	,326350.10602358	,5057.4973917227	,1278.		
24	,675515.11731511	,326325.75919459	,5057.7643214729	,1279.		
25	,675490.10657356	,326326.38406258	,5056.8162735724	,1280.	75.60	0.40
25	,675465.09069247	,326326.99626439	,5054.6573286646	,1281.		
25	,675440.11575066	,326327.77519704	,5055.3060039284	,1282.	42.90	0.30
25	,675415.23245618	,326328.35659068	,5054.7819976545	,1283.		
25	,675390.21736946	,326328.90513771	,5053.9323410250	,1284.		
25	,675414.50150548	,326303.33324060	,5053.9682969309	,1286.		
25	,675439.50481441	,326302.78924931	,5054.5568272439	,1287.		
25	,675464.49202803	,326301.97878561	,5057.2632633446	,1288.	81.70	0.40
25	,675463.75917934	,326276.94620972	,5055.6444636932	,1291.		
25	,675489.66739419	,326276.28598355	,5056.1837669202	,1292.		
26	,675489.93558223	,326301.09775791	,5056.7961898780	,1293.		
26	,675514.35372843	,326300.75022314	,5057.4334808366	,1294.	174.00	0.50
26	,675513.57599280	,326275.75765997	,5056.8832566567	,1295.		
26	,675539.99515154	,326275.04975866	,5057.0264477912	,1296.		
26	,675540.16996712	,326299.86792296	,5059.1882511072	,1297.		

ARA 23 RESULTS: Cs-137 (pCi/g) by location
α/ρ=0.059, ρ(soil)=1.6 g/cm^3
RELAXATION LENGTH= 4.2 INCHES

CPP RADIOCHEMISTRY GROUP 9/97
FIELD MEASUREMENTS: SJ HILL, BK HARRIS, KJ OLTMANNS, CP OERTEL
DATA ANALYSIS: CP OERTEL

Point ID	North	East	Elevation	Descriptor	Cs-137 (pCi/g)	Error (1s)
26	,675541.29927698	,326324.90162447	,5058.1446619591	,1298.	169.00	0.53
26	,675565.58871057	,326349.37266433	,5058.5898463271	,1299.	126.00	0.50
26	,675585.25058899	,326324.62957063	,5058.8208650601	,1300.		
26	,675564.32204256	,326299.11255797	,5057.8614102867	,1301.		
26	,675588.31413677	,326299.02088114	,5057.7072712387	,1302.		
27	,675589.50945470	,326324.07845903	,5059.7250942258	,1303.	132.00	0.50
27	,675590.50402335	,326348.94762872	,5058.3801053608	,1304.		
27	,675614.58413872	,326323.48267049	,5056.9522972876	,1305.		
27	,675615.57873719	,326348.08228487	,5058.6661026571	,1306.	141.00	0.50
27	,675616.62033660	,326373.53779745	,5058.6318886144	,1307.		
27	,675640.35213145	,326347.22788944	,5056.8495215471	,1308.		
27	,675641.09432179	,326372.58238596	,5057.4631311187	,1309.	129.00	0.50
27	,675641.82284302	,326396.97200332	,5058.8024605272	,1310.		
27	,675667.06439947	,326396.80615269	,5056.7339624071	,1311.		
27	,675667.74898578	,326422.21793026	,5058.3275383701	,1312.		
28	,675692.71975652	,326421.12422328	,5056.6719604139	,1313.		
28	,675693.75360784	,326446.30146174	,5056.6519262633	,1314.		
28	,675668.43293205	,326446.97426635	,5059.5355243493	,1315.	64.80	0.35
28	,675668.48336591	,326471.67965242	,5056.6848630154	,1316.		
28	,675643.70157531	,326472.32720986	,5056.8829194608	,1317.		
28	,675644.61864215	,326498.16097358	,5055.6144081898	,1318.		
28	,675619.76806771	,326498.38888748	,5055.7250792041	,1319.		

ATTACHMENT 2

LOCKHEED MARTIN

Lockheed Martin Idaho Technologies Company

INTERDEPARTMENTAL COMMUNICATION

Date:	September 4, 1997		
To:	N. E. Josten	MS 2107	6-7691
From:	R. J. Gehrke/R. G. Helmer	MS 2114	6-4155/6-4157
Subject:	CONVERSION OF ARA-23 DATA TO CONTAMINATION LEVELS - RJG-16-97/RGH-39-97		

In response to a request, we have generated a factor to convert count rates from the TSA plastic scintillator mounted on the Vehicle Roadway Monitor, VRM, system to contamination levels. This system was used recently for a survey of the ARA-23 area, site of the 1961 SL1 accident at the INEEL. It MUST BE EMPHASIZED that there are several assumptions and approximations involved in creating this conversion factor and that some measurements should be made with this system on calibrated sources in order to validate these results. So that you can understand the potential limitations of these results, the various steps involved are described.

The initial step was the modeling of the response of a 12"x12"x1.5" plastic scintillation detector which has been used for other surveys of radionuclide activities. This modeling was done using the Monte Carlo electron and photon transport code CYLTRAN. Although this detector is rectangular, the limitations of CYLTRAN required that it be represented as a right circular cylinder, but for the earlier uses of the detector this was not a serious limitation. This detector is used with the 12"x12" surface facing the soil and it has a lead shield around the edges of the detector. This modeling has been done for a variety of source (i.e., area of contamination) sizes, both in horizontal direction and depth in the soil as well as for different soil-detector distances. For the cases of interest here, the modeling was done for photons with an energy of 662 keV, as obtained from ^{137}Cs and for a soil-detector distance of 1 meter. Each such calculation gives the detector response as a spectrum giving the number of events as a function of the amount of energy deposited in the plastic scintillator. The energy deposited is not the full energy of the photons because, when the original photon interacts with the detector, secondary photons are produced and they have a high probability of escape from the detector.

A low-level discriminator in the detector electronics cuts off, or discards, all of the events which deposit less than a particular energy. It is expected that this cutoff lies between 50 and 150 keV for the TSA detector. This range will correspond to a range of approximately 2 in the measured count.

In this work to support the ARA survey, it has been assumed that the ^{137}Cs activity is uniformly distributed down to a depth of 4 inches, 10.16 cm, and over a large area. The detector response was computed for several source depths between 0 and 4 inches and these were combined to give the desired response for a uniform distribution down to 4 inches. (Calculations were also done to give the response if the contamination is all on the surface.)

For this 12"x12"x1.5" plastic scintillator, the results can be reported in the following way. The percentage of the 662-keV γ rays emitted from a uniformly distributed source 14 meters in diameter and 10.16 cm into the soil that deposit more 50 keV of energy in the detector is 0.00954. If the electronic cutoff on the detector is 150 keV, this percentage is 0.00547 or at 100 keV, about 0.0068. If we assume the best value for this cutoff for the TSA detector is 100 keV, but allow it to be anywhere from 50 to 150 keV, this percentage is 0.0068 +0.0027-0.0013.

In order to convert these results to the TSA detector, we have compared the results from the modeling for a 12"x12"x4" detector with the 1.5" thick one discussed above. The effect of the added thickness is to absorb more of the secondary photons and thereby move some events up past the cutoff energy. The computed increases in the above percentages of events above the two cutoffs are given by the following factors:

2.1 for a cutoff of 50 keV and
2.2 for a cutoff of 150 keV.

We expect the loss of secondary photons to be somewhat larger for the TSA detector than calculated for the 12"x12"x4" detector due to it being only 4" across. Therefore, we have used a factor of 1.8±0.3 in the following calculations.

The volume of the TSA scintillator is 11% larger than the 12"x12"x4" detector, so the efficiency is assumed to be larger by this amount.

In order to proceed, we must assume that the TSA plastic scintillator has no inherent differences from our 12"x12"x1.5" plastic scintillator, except those due to the difference in size. This is a very reasonable assumption, but we have no experimental information to verify it. The percentage of 662-keV photons that we might expect to produce events above a cutoff of 100 ± 50 keV in the TSA system would then be estimated as follows:

value for 12"x12"x1.5" detector	0.0068% +0.0027-0.0013,
corrected to 12"x12"x4" detector	0.0122% + 0.0053-0.0031, and
corrected for 11% added volume	0.0136% +0.0059-0.0034.

ATTACHMENT 3

ARA for other Depths

calc. depths cm	calc. uniform to cm	calc. uniform to inches	% of cts above lake V cutoff & uniform to	Mass of sample (g)
1.3	2.6	1.0	0.0109% $^{+36}_{-18}$	5.87×10^6
3.8	5.1	2.0	0.00917% $^{+33}_{-16}$	1.18×10^7
6.4	7.7	3.0		
8.9	10.2	4.0	0.0068% $^{+27}_{-13}$	2.36×10^7

$$\text{mass} = \pi r^2 d \rho = 1.5 \pi r^2 d = 2.309 \times 10^6 d$$

uniform to	cts/sec.	γ's/sec.	dis/s ^{137}Cs	pCi	pCi/g	$\frac{pCi}{g} \times$ depth (in.)
1"	100	9.17×10^5	1.08×10^6	2.92×10^7	4.97	5.0
2"	"	1.70×10^6	1.29×10^6	3.49×10^7	2.96	5.9
4"	"	1.47×10^6	1.73×10^6	4.68×10^7	1.98	7.9

1 Ci = 3.7×10^{10} d/s

1 nCi = 37 d/s

1 pCi = 0.037 d/s

ATTACHMENT 4

X-Sender: rhz@axp1.inel.gov
X-Mailer: Windows Eudora Light Version 3.0.1 (32)
Date: Thu, 25 Sep 1997 16:19:51 -0600
To: GSense@srv.net
From: Richard Helmer <rhz@inel.gov>
Subject: ARA data on source depth
Mime-Version: 1.0
X-UIDL: ccd32b7d87250eac9a9de166dc4117dd

Nick,

Bob Gehrke called and said that the ratio of the peak areas for the K x ray and gamma ray from 137Cs was 0.20 on the average and ranged from 0.15 to 0.25. (All numbers are approximate at this point. He was still counting the last spectrum.) My previous Monte Carlo runs for this Ge detector and for large diameter (120 cm) disk sources at various depths can be interpolated and processed to give the following X/gamma ratios:

all of source at depth of (cm)	X/gamma ratio
on surface	0.58
0.3	0.43
0.9	0.22
1.5	0.117
2.1	0.061
2.7	0.032

So, the "centers" of the sources have to be near 1.0 cm.

source uniform down to (cm)	X/gamma ratio
1.2	0.32
1.8	0.26
2.4	0.21
3.0	0.17
15.2	0.077

So, a uniform distribution would need to extend down to about 2.5 cm (1**).

If the radioactivity were wind blown and then washed down into the soil, one would expect more near the surface (although eventually it might all be washed down some minimum distance). So, I tried a couple of trianguler distribution: of which the following is the most interesting:

9/25 at 0.3 cm
7/25 at 0.9 cm
5/25 at 1.5 cm
3/25 at 2.1 cm
1/25 at 2.7 cm

which gives an X/gamma ratio of 0.25.

A suggestion, based on Bob's comments. The X/gamma ratios near 0.15 may be in regions were the radioactivity was buried near 1.2 cm when items were dragged to the burial area. The X/gamma ratios near 0.25 are for wind blown material that has been washed down to give a distribtuion near the above trangular distribution. In the latter case, over 90% of the activity would removed with the top 2.6 cm, or 1 inch, of soil.

Things are, of course, much more complex than this, but this is an idea to start any discussion.

See you,

Dick

Richard Helmer
Email:rhz@ienl.gov
Phone:(208)526-4157
Lockheed Martin Idaho Technologies Co.
Idaho National Engineering and Environmental Laboratory

ATTACHMENT 5

LOCKHEED MARTIN

Lockheed Martin Idaho Technologies Company

INTERDEPARTMENTAL COMMUNICATION

Date: September 30, 1997

To: Distribution

From: R. J. Gehrke RJG MS 2114 6-4155
R. G. Helmer RGH. MS 2114 6-4157

Subject: PROGRESS IN IN SITU MEASUREMENTS - RJG-17-97 AND RGH-50-97

During the past year, we have been involved in a variety of activities related to the in situ measurements of contamination levels in soils. This has included LDRD work on the calibration of radiation detectors with computer modeling by means of a Monte Carlo photon and electron transport code as well as related measurements supported, in part, by other programs. This work has involved three types of detectors: two Ge semiconductor detectors, a plastic scintillator, and an array of six CaF_2 detectors. Laboratory measurements have been made at the Test Reactor Area and field measurements have been done at Mound Laboratory, Savannah River Site, and very recently ARA-23 at the INEEL. (The modeling related to the ARA work is not discussed here.)

The enclosed report has been prepared to allow all interested parties to see the range of work that has been done and to provide a basis for discussing what still needs to be done. No site-specific results are discussed in the report.

We feel that this effort has been very successful in establishing a general understanding of the capabilities and limitations of in situ measurements with these three detector systems. For example, the Ge detector measurements at ARA 23 of the relative intensity of the 32-keV x ray and the 661-keV γ ray from the ^{137}Cs ground contamination gives an estimate of the depth distribution, as well as giving information on the total amount of ^{137}Cs present.

It should, however, be emphasized that these systems and analysis methods have not been developed to the point that they can be used routinely for quantitative in-field measurements. (The plastic scintillator can be used routinely for survey work, but the conversion of the measured count rates to contamination levels is not routine.) Currently, essentially all of the data must be analyzed after the fact and special modeling calculations are often required. We suggest that two years of adequately funded work is needed to allow quantitative in-field analysis. The first year would be used, in part, to accumulate the necessary measurement data to verify the modeling work, as well as doing more precise modeling. The second year would then be used to used to put this information in a form to allow the creation of software and data files to provide in-field analysis and interpretation of the measurements.

The following list gives brief statements of the various tasks that should be carried out in order to fully utilize the capability of these three detector systems. We have not included here any other types of detectors/sensors, but we have included the closely related plastic scintillator mounted on a HumVee, the Vehicle Roadway Monitor, for the assay of large areas.

1. Geometric deconvolution

Some of these detectors view a large area of the ground, so only a small spot of radioactivity will influence a large area on a survey map. Since the viewing angle, or spatial resolution, of a detector can be determined from calculations or measurements, it would be possible to remove some of this effect and thereby make the survey maps more closely represent the spatial distribution of the radioactivity in the soil. (This work would be outside the area of expertise of the authors of this letter.)

2. Critique of ISOCS calibration and software for Ge detectors

We need to make several types of measurements as well as new modeling calculations to test the accuracy and range of usefulness of the commercial ISOCS software.

If the ISOCS calibration and software are not sufficiently accurate for our uses, it may be possible to improve this method by collaboration with the supplier, or other analysis methods will need to be developed.

3. Plastic scintillator efficiency and spatial resolution

So far we have relied primarily on the modeling and an estimate of the electronic cut-off to determine the efficiency of the 12"x12"x1½" plastic scintillator. We need to make measurements of the count rates for calibrated sources of selected sizes of ^{137}Cs and ^{228}Th or ^{232}Th to verify the deduced efficiency.

Until the geometric deconvolution methodology noted above is completed, and as test data for checking such a computer code, we need to measure the response of the plastic scintillator as it passes over sources of various sizes to determine its spatial resolution. We can now do this with ^{137}Cs sources with lengths of 10, 60, 120, and 240 cm.

4. CaF_2 detector modeling

In the field this detector/sensor includes an array of six 3"x3" detectors. So far, we have only modeled a single detector, and that as a circular disk. We need to improve the modeling to properly represent the six detector array.

There may be an inconsistency between some measurement results for the plutonium isotopes from the Ge semiconductor detector and the CaF_2 detector. This may need to be explored by more modeling calculations or measurements.

Although this array is useful for the measurement of the L x rays from the plutonium isotopes at about 16 keV and the ^{241}Am γ ray at 59 keV, we have shown experimentally that it is not useful for the 32-keV x ray from ^{137}Cs due to the large spectral background from the associated 661-keV γ ray. We would like to explore, via modeling calculations, the possibility of improving the design of the detector mounting for such measurements.

5. TSA plastic scintillator

We have made some estimates of the efficiency of the TSA plastic scintillator on the Vehicle Roadway Monitor, VRM. For this system some new modeling calculations are needed. Also, an extensive set of measurements are needed in order to verify the modeling as well as to determine the influence of the shielding of the detector by the VRM itself.

6. Publications and symposia

With the combination of the Warthog system, the mapping capability, and the complimentarily of the three detector systems, this system has great potential. This potential needs to be publicized. Therefore, we will promote the publication of two or three journal articles as well as presentations at appropriate technical meetings.

Enclosure

Distribution

M. V. Carpenter (3), MS 2107
K L. Falconer, (w/o Encl), MS 3921
J. K. Hartwell, MS 2114
R. A. Hyde, MS 3765
K. M. Kostelnick, MS 3710
J. A. Lake, (w/o Encl), MS 3860
J. W. Mandler, MS 2114
R. N. Snelling (w/o Encl), MS 2213
F. L. Webber, MS 3953
P. L. Wichlacz, MS 2213

25 September 1997

Progress on Hyde LDRD and Related Activities

Summary

The main goal of this work is to develop the knowledge which will allow one to convert the count rates observed in three different detector/sensor systems to the activity level of certain radionuclides that are commonly found in the soil in field measurements of contamination. The detector systems of current interest are (1) plastic scintillator which is an excellent general γ-ray detector but gives almost no information about the radionuclides present, (2) CaF_2 which is useful for very low energies (specifically around 15 keV), and (3) Ge semiconductor detectors which are especially useful if one wishes to identify and quantify the radionuclides present.

A great deal of experience has been gained this year in the area of in situ measurement of radionuclides with these three types of γ- and x-ray detectors. By combining the results of modeling calculations with the detector development and in situ measurements, we have been able to develop an understanding of the merits and limitations that are related to each type of detector system.

This report describes what R. J. Gehrke and R. G. Helmer have done during FY97 in the modeling of detector efficiencies and using this information to estimate activity concentrations in situ. It is expected that part of this material will be polished and expanded to create a journal article.

Organization of Technical Session at American Nuclear Society Meeting

Bob Gehrke organized a Technical Session at the June 1997 meeting of the American Nuclear Society entitled Status of Accurate Methods for Peak Efficiencies of Gamma-ray Spectrometers for Extended Sources. The Session was organized to provide support for our efforts under this LDRD and related work. The Session was very successful in that it included eleven papers presented by the top experts for this type of work from the United States and six European countries (i.e., Finland, France, Germany, Norway, Romania, and Slovenia). After the presentations, a panel discussion was held in which the participants shared ideas informally and discussed their plans for future work in this area.

Monte Carlo Modeling with CYLTRAN

For all of the detectors considered here, we have used the Monte Carlo electron and photon transport code CYLTRAN to model the detector response. We had previously used this code with excellent success for many years for modeling of the response of Ge semiconductor detectors and NaI(Tl) scintillation detectors.

As background, it is useful to comment on what the Monte Carlo code provides and its limitations. For each specific calculation one provides as input two files of information. One is a file of information (i.e., a list of cross sections) on how electrons and photons (i.e., γ rays and x rays) interact with the different chemical elements that are present. The second file describes the physical

geometry of the source, detector, and other materials as well as the γ-ray energy, the energy bins (called channels in an measured spectrum) in which the events are tallied for the energy lost in the detector volume, and the number of photons to be emitted.

The code tracks each γ ray as it travels through space and interacts with atoms in the various materials present. The electrons and secondary photons produced in these interactions are also tracked until all of their energy has been dissipated in the various materials or escaped out of the physical space included in the model.

For interactions in the detector volume, the code produces a tally of the number of events in each energy bin; that is, it provides an energy-loss spectrum. Since a measurement system does not directly measure the energy deposited in the detector, the calculated spectrum will differ to some extent from a measured spectrum even if the modeling is done without any approximations or errors. For a Ge semiconductor detector, which has a very linear response (i.e., the amplitude of the signal from the detector is proportional to the energy deposited) and very good energy resolution (i.e., any observed peaks are very narrow), the differences will often be very small. In contrast, a plastic scintillator has very poor energy resolution , so any peaks that occur in the Monte Carlo calculated spectrum will be smeared out and only marginally recognizable in the corresponding measured spectrum.

The CYLTRAN code requires that the geometry be axially symmetric, that is, each piece is either a right circular cylinder and annulus. Therefore, rectangular objects must be approximated as circular objects.

The geometrical description of the source-detector system for CYLTRAN can be as detailed as one wishes, as long as it has cylindrical symmetry. For the three types of detectors discussed here, each geometrical description includes the following:

the sensitive volume of the detector,
the mounting materials around the detector,
the entrance window or cover over the front of the detector,
the shielding to reduce the response to photons from locations other than the desired source,
the air between the source and detector, and
the soil.

The peak efficiency, ϵ_p, is simply the ratio of the peak counts to the photons emitted and it will depend on the photon energy and the source-detector geometry.

ISOCS and RJG5 Ge detector

Our LDRD plans included as a major effort this year, the evaluation of the commercial software known as ISOCS from Canberra Industries for computing the effective efficiency for a specific, Canberra-calibrated, Ge semiconductor detector as a function of the γ-ray energy. The selling point of ISOCS is that it can compute this efficiency for a large variety of user defined configurations of the radioactivity (e.g., surfaces, boxes, or pipes).

The ISOCS calibration by Canberra consists of measurements of the peak efficiency at several photon energies for point sources at several locations. These data are supplemented by a large number of Monte Carlo calculations of the peak efficiencies for other photon energies and locations. All of these data are then summarized by a set of polynomials. Additional Canberra software can then use these polynomials and photon attenuation cross sections to compute the peak efficiency for many specific user-defined source volumes including the attenuation in materials in the source volume or between the source and the detector.

Since Canberra did not deliver this software until May, this portion of our work had to be deferred. Currently tests are being carried out to compare the results that are obtained for the efficiencies for point sources from (1) measurements with calibrated sources, (2) the CYLTRAN Monte Carlo photon and electron transport code, and (3) ISOCS. The initial tests emphasized low-energy (e.g., about 100 keV) γ rays. Although this may be below the optimum energy for ISOCS, it is a region that can be used to check the source-detector distance which is an important parameter in the CYLTRAN calculations. This effort includes the construction of a holder for point sources in front of the detector for the detector (known as RJG5) that was calibrated by Canberra for ISOCS. A second source holder for point sources was made to allow the source to be moved over a 90° arc at 1 meter from the detector.

Four large-area sources of ^{137}Cs for use in additional measurements to test ISOCS have been prepared by Analytics, Inc. and delivered. When used together these cover an area of 1.2 meter x 1.2 meter or 0.6 meter x 2.4 meters.

RJG4 Ge detector

While waiting for the ISOCS Ge detector, a large number of CYLTRAN runs were made to explore a variety of measurement parameters for in situ counting with a Ge detector. For these tests, the modeling was done for the detector RJG4 which is almost identical to the ISOCS detector, RJG5. This detector was mounted inside a shield which extended about 2.75" beyond the detector housing and usually the shield is 6" from the soil. The modeling was done for the following variables: diameter of disk source on soil surface, depth of a disk source in the soil, composition and density of soil, and displacement of point source from detector axis. The latter calculations were compared with a set of measurements. Also, a series of runs was made to explore the information that could be obtained concerning the radial extent and depth distribution of ^{137}Cs when the 32-keV K x rays are observed in addition to the 662-keV γ ray. The conclusions from these modeling calculations, along with some of the data, follow.

Influence of Shield

For a ^{137}Cs source with diameter of 1 meter on the soil surface, removal of the shield would increase the count rate in the full-energy peak of the 661.6-keV γ ray by a factor of 2.95 (8). In contrast, for a point source on, or near, the detector axis the count rate would be unchanged because the shield does not block any photons.

Therefore, the comparison of counts with and without the shield would give some immediate information of the lateral distribution of the source material.

Source-Detector Distance

For measurements in the field, it will often be difficult to control the source-detector distance. Therefore, it is desirable to know the influence of the source-detector distance on the count rate. Calculations of the peak efficiency, ϵ_p, at 660 keV were made for two distances and two source diameters for a source on the soil surface.

	Relative peak count rate	
Source-detector distance (cm)	Point source	60-cm diameter source
15.2 (6")	2.05	1.04 (3)
22 (8.66")	≡1.00	≡1.00

For the point source, the change is simply the result in the change in the solid angle subtended by the detector from the source point, that is, $(22.0/15.2)^2$. In contrast, for the large source as the distance is increased, the decrease in solid angle is compensated for by the fact that the detector sees a larger source area.

There are two interesting conclusions from these data. First, for field surveys changes in the source-detector distance are not important for the determination of the source activity level for large area sources. Second, one can change the source-detector distance and use the variation in the peak count rate to determine if the source is more nearly a point source or a large area source.

Influence of Depth in Soil

If the source is distributed down into the soil, there are three factors that influence the observed count rate. For a given specific activity of the source, as the depth increases (1) the distance to the detector increases, so the count rate decreases; (2) the detector views a larger source area, so the count rate increases; and (3) the photon attenuation in the soil increases, so the count rate decreases.

As a function of the depth in the soil, the peak efficiencies (or counts) were computed for 16-keV photons of interest in measuring the plutonium isotopes and 660-keV photons of interest for ^{137}Cs with the following results:

Photon energy (keV)	Source diameter (cm)	Depth in soil (cm)	Relative peak count
16	160	0.05	≡1.000
		0.15	0.440
		0.25	0.165
		0.35	0.077
		0.45	0.031
660	60	0	≡1.000
		2	0.82
		4	0.61
		8	0.34
		16	0.081

From these data it is clear that at 16 keV for a source that is distributed uniformly with depth, the count rate will depend on the material in the first 0.2 or 0.3 cm. If the active material is covered with up to about 0.3 cm of clean soil, the activity can sill be observed, but the activity level will need to be considerably stronger than for surface contamination.

For photons of 660 keV, the count rate will have significant contributions down to 10 to 16 cm and a cover of a few cm of clean soil will not be a serious hindrance.

Influence of Source Diameter

For a ^{137}Cs source (i.e., 662-keV γ rays) uniformly distributed on the soil surface, the peak count, or efficiency, was computed as the source diameter increased. The sources all have the same specific areal activity, or disintegrations per cm^2; that is, the total source activity increased as the square of the source diameter.

Source diameter (cm)	Relative peak count
20	0.342 (14)
30	0.638 (19)
40	0.93 (3)
52	0.99 (3)
56	1.00 (3)
60	0.99 (2)
64	≡1.00 (2)
80	1.02 (3)
100	1.04 (2)
140	1.00 (2)

These data show that for sources larger than 40 cm in diameter, the photons from the outer portion of the source are blocked by the shield.

Influence of Soil Composition and Density

Modeling calculations were done to determine if the soil composition had any discernable influence and to verify the expected density influence. These CYLTRAN calculations were for 662-keV photons and a 60-cm diameter source.

Some of our early runs were done with the soil represented as simply SiO_2. But, the recent ones were done with a Beck soil composition with a water content, by weight, of 0%, 10%, or 20%. For the 10% water content, the chemical composition of the Beck soil, by weight, is SiO_2 67.5%, Al_2O_3 13.5%, H_2O 10%, Fe_2O_3 4.5%, and CO_2 4.5% which gives the elemental composition of O 55.8%, Si 31.6%, Al 7.2%, Fe 3.1%, C 1.2%, and H 1.1%.

For sources at depths of 0, 4, and 8 cm, the results are:

Source depth (cm)	Soil composition	Density (g/cm^2)	Relative peak count - at one depth
0	SiO_2	1.5	0.98
	dry Beck	1.5	1.02
	20% H_2O Beck	1.5	1.00
4	SiO_2	1.5	1.00
	dry Beck	1.5	1.00
	20% H_2O Beck	1.5	0.99
	20% H_2O Beck	2.0	0.78
8	SiO_2	1.5	0.98
	dry Beck	1.5	1.03
	20% H_2O Beck	1.5	0.98
	20% H_2O Beck	2.0	0.64

The values at a depth of 0 cm must be the same since the soil has no influence on the full-energy peak; they are the same. At the other two depths, the three values for a density of 1.5 g/cm^2 all agree, so these three soils are equivalent for these 662-keV γ rays.

The higher density increases the attenuation and gives the lower relative peak count, as expected. However, if the results are reported in the typical form of pCi/g, the density cancels out, except for volume sources very close to the detector.

Peak Efficiency vs Photon Energy

ϵ_p was calculated by CYLTRAN for sources on the surface of the soil with source-detector distance of 22 cm. The values with source diameters of 0 and 10 cm should be equivalent since the

shield will not attenuate any of the photons emitted in the direction of the detector. For comparison some measured values are also given.

Source diameter (cm)	Photon energy (keV)	ϵ_p (%)	
10	32	0.280	
0	121	0.238	(measured 0.233)
0	344	0.0687	(measured 0.0703)
10	583	0.0328	
10	662	0.0303	
0	1408	0.0124	
160	16	0.020	
120	32	0.0209	
120	662	0.00245	

Peak Efficiency vs Off-axis Distance

A series of measurements was made with a calibrated ^{152}Eu point source and the peak efficiencies for the γ rays at 121, 344, and 1408 keV were determined. This source was counted on the detector axis at a source-detector distance of 22.86 cm and then displaced perpendicular to this axis, in the "y" direction, by various distances from 2.5 to 30.5 cm.

CYLTRAN calculations were made for these three energies and the same source-detector geometries. The comparison of measured and modeled ϵ_p values indicates excellent agreement as shown in the table below.

The main approximation in the modeled geometry was that the end of the detector shield was simplified from the actual curved surface to a few square steps. This difference, as well as any difference of the position of the detector with respect to the shield makes a significant difference as the source passes out of direct view of the detector, say from 15 to 25 cm. However, there is still good agreement at y = 30 cm and E_γ = 1408 keV where all these photons are penetrating the shield.

Photon energy (keV)	y positron (cm)	ϵ_p (%) measured	modeled
121	0	0.233	0.238
	2.5	0.233	0.236
	5.1	0.224	0.228
	10.2	0.196	0.197
	15.2	0.122	0.104
	20.3	0.048 6	0.0363
	25.4	0.000 18	0.0032

	30.5	0.000 007	0.000 05
344	0	0.070 3	0.068 7
	2.5	0.069 6	0.067 5
	5.1	0.062 4	0.064 6
	10.2	0.059 2	0.057 1
	15.2	0.038 8	0.033 8
	20.3	0.014 0	0.011 2
	25.4	0.000 04	0.000 77
	30.5	-	0.000 001
1408	0	0.012 8	0.012 4
	2.5	0.012 8	0.012 1
	5.1	0.012 5	0.011 7
	10.2	0.011 0	0.010 5
	15.2	0.008 34	0.007 32
	20.3	0.003 06	0.003 22
	25.4	0.000 370	0.000 466
	30.5	0.000 236	0.000 256

This excellent agreement is an illustration of the good quality of the CYLTRAN calculations.

Information about Source Distribution from 32-keV K x rays of ^{137}Cs

An in situ ^{137}Cs spectrum taken at the Savannah River Site had a measurable peak at 32 keV from the K x rays. This provided an opportunity to determine what information could be extracted about the distribution of the ^{137}Cs in the soil from just the count rates for this 32-keV x-ray peak and the 662-keV γ-ray peak. The measured spectrum gave count rates of 23.33 (24) counts per second at 662 keV and 1.38 (9) at 32 keV.

In spite of the fact that there is an infinite number of possible source distributions that would match these data, it is of interest to determine what distributions can be ruled out. Six simple possible distributions were considered. In addition, the influence of a thin layer of clean soil on top of the source was considered. The six basic activity distributions were:

1. small diameter (10 cm) source on the surface of the soil
2. large diameter (120 cm) source on the surface of the soil
3. small diameter source uniform down to 3.6"
4. large diameter source uniform down to 3.6"
5. small diameter source uniform down to 6"
6. large diameter source uniform down to 6"

The CYLTRAN calculations were made with disk sources of these two diameters placed at several depths in the soil. The peak efficiencies at the various depths were combined to give the average peak efficiency for the two "uniform to x" distributions.

The conclusions from this one spectrum were:

a. The ^{137}Cs was not primarily on the surface. If it were on the surface, the 32-keV peak count rate would have been larger by a factor of about 10.
b. A small diameter source uniform to 3.6" is not a good match; the 32-keV peak should still be larger by a factor of 2.4.
c. A large diameter source uniform to 3.6" gives fairly good agreement since the activity level computed from the two peaks differ only by a factor of 1.6. (See item f below for the influence of a thin cover of clean soil.)
d. A small diameter source uniform to 6" is also fairly reasonable with the ratio of the activities of 2.0. (See item f below for the influence of a thin cover of clean soil.)
e. The large diameter source uniform to 6" is very good, with the ratio of the activities computed from the two lines differing by only a factor of 1.3.
f. For cases c,d and e, the modeled 32-keV peak is too strong, but this could be reduced with a layer of clean soil on top of the contaminated soil. For item c, only 0.5 cm of clean soil would make the activities calculated from the two peaks agree; and for item d, 0.75 cm of clean soil would give a match. For item e, much less clean soil would give an exact match.

These measured data can also be used to get some limits on the ^{137}Cs activity, i.e., disintegrations per second per gram of soil. These values extend over a range of 17 from 10.5 dis/s-g for a 120-cm diameter source uniform to 6" to 178 dis/s-g for a 10-cm diameter source uniform to 6" with 0.75 cm of clean soil on top. Therefore, a scan which can define the horizontal extent of the source would be necessary for a more accurate quantitative interpretation of the Ge detector results.

Plastic scintillator

We have also proceeded with the expansion of our knowledge concerning the other detectors included in this project starting with the 12"x12" x 1.5" plastic scintillator that has been used for several surveys.

Modeling with the CYLTRAN Monte Carlo code has included determining how the count rate in the detector varies with the electronic cut-off, the γ-ray energy, the distance from the soil, and the distribution of the activity in or on the soil. The geometry used in the modeling for this detector included the lead shield and a representation of the support frame. All of the items are rectangular, so for the CYLTRAN modeling, they had to be represented by the circular objects with the same area. This will not introduce any significant errors. (Calculations with another Monte Carlo code that can treat rectangular objects indicates the difference between the results for the circular and rectangular shapes is ~ 1%.)

Spectra and electronic cutoff

This detector converts the energy from the incident photons to light radiation and the amount of light leaving one 12" x 1.5" end surface is measured with a multiplier tube and the associated electronics. The light is reflected from the other five surfaces, so that most of it exits in the direction of the photomultiplier. The detector is covered with an opaque material so that light from external sources can not get into the scintillator.

The response of the plastic scintillator was computed for photons of 660 keV, that is, essentially the energy for the γ rays from ^{137}Cs. The figure shows the energy-loss spectra directly from CYLTRAN which are for a 10-cm diameter disk source on the soil surface and at 13.7 cm deep in the soil. Although there is a peak in the former spectrum at about 460 keV, the photon scattering in the soil has almost eliminated this peak in the latter spectrum. The process of converting the energy lost in the detector to light is a statistical one with a very broad distribution, so the peak in the figure will be broadened in the measured spectrum to the extent that one should not expect to see peaks in the measured spectra.

In measured spectra, electronic noise will also contribute to the low-energy portion of a spectrum. The energy range over which this noise is a significant contribution will depend on several parameters of the detector system including the quality of the optical coupling between the plastic and of the photomultiplier. For measurements, this noise is eliminated from the spectrum by electronically rejecting all pulses that are below some specified voltage. For the measurements that have been made so far, it has been determined that this electronic cutoff was at about 150 keV. (For the in-field measurements, the pulses above the electronic cutoff are counted in a scaler, so the spectrum is not obtained.) Due to the large rise at the lower energies, as shown in the figure, the observed count rate from a ^{137}Cs source can vary significantly depending on the electronic cutoff. The next table gives the calculated fractions of the 660-keV γ-rays emitted from sources of 10-cm and 120-cm diameters on the soil surface and buried in the soil that deposit more than 50 or 150 keV in the detector. Over this range the electronic cutoff can vary the observed count rate by a factor of up to 2.0.

Source		Fraction of emitted γ rays depositing in detector (%)			
Diameter	Depth in soil	Disk source		Uniform source to 15.2 cm	
(cm)	(cm)	50 keV	150 keV	50 keV	150 keV
0	0.0		2.181 (10)		
10	0.0	3.455	2.141		
	1.5	3.365	1.934		
	4.6	2.593	1.376		
	7.6	1.915	0.972	2.044	1.081
	10.7	1.369	0.663		
	13.7	0.979	0.462		
120	0.0	1.277	0.834		

1.5	1.214	0.727		
4.6	0.922	0.509		
7.6	0.679	0.354	0.734	0.402
10.7	0.496	0.247		
13.7	0.358	0.173		

It is of some interest that, since there are no peaks in these spectra, it is difficult to experimentally determine the energy correspond to the electronic cutoff. This ambiguity will introduce a small uncertainty in the conversion of the measured count rate to the radionuclide activity concentration.

The information in the above table can be presented in another form as the "massometric efficiency". The soil density is 1.5 g/cm^3.

Source Diameter (cm)	Uniform to (cm)	(Mass of source) x (Fraction of emitted γ rays depositing in detector (%)) 50 keV	150 keV
10	3	1189	684
	6	2106	1170
	9	2783	1513
	12	3266	1748
	15	3612	1911
120	3	61,785	37,000
	6	108,709	62,905
	9	143,266	80,921
	12	168,509	93,492
	15	186,729	102,297

The massometric efficiency approaches an asymptote which is about 10% larger than the value given for the source which is uniform to 15 cm.

Dependence of response on γ-ray energy

For the measurements of radionuclides other than ^{137}Cs, one needs to know how the observed count rate will vary as the γ-ray energy varies. Looking forward to the possibility of measuring ^{232}Th or ^{228}Th levels in equilibrium with their daughters, we determined, with CYLTRAN, the detector response for γ-rays of 240 and 2610 keV, where these radionuclides have strong γ rays. Also, one value was measured at 1250 keV, the mean γ-ray energy for ^{60}Co.

As expected, the influence of the electronic cutoff is much smaller for the 2610-keV γ rays, the variation has a minimum of 1.5 for the same cases as shown in the above table for 660 keV. However, for 240-keV γ rays, the number of events above 50 keV are as much as 26 times larger

than the number above 150 keV. As indicated by the data in the table below, the energy of the electronic cutoff will be important in the count-to-activity conversion for any radionuclide with strong γ rays below, say, 350 keV.

The modeled spectra were calculated for γ rays emitted from disk sources of 10-cm and 120-cm diameters on the soil surface and at five depths from 1.5 to 13.7 cm. The depths were equally spaced and if the five values are averaged the result represents a source that is uniformly distributed down to 15.2 cm or 6 inches.

Source Diameter (cm)	Depth in soil (cm)	Fraction of emitted γ rays depositing in detector (%) Disk source 50 keV	150 keV	Uniform source to 15.2 cm 50 keV	150 keV
		E_γ = 240 keV			
10	0.0	3.103	0.297		
	1.5	2.758	0.215		
	4.6	1.807	0.120		
	7.6	1.120	0.060	1.358	0.090
	10.7	0. 690	0.035		
	13.7	0.417	0.018		
120	0.0	1.106	0.834		
	1.5	0.930	0.727		
	4.6	0.576	0.509		
	7.6	0.351	0.354	0.441	0.028
	10.7	0.215	0.247		
	13.7	0.132	0.173		
		E_γ = 1250 keV			
10	0.0	3.021	2.188		
		E_γ = 2610 keV			
10	0.0	2.423	1.871		
	1.5	2.539	1.893		
	4.6	2.143	1.512		
	7.6	1.759	1.215	1.796	1.266
	10.7	1.411	0.950		
	13.7	1.129	0.761		

120	0.0	0.949	0.744		
	1.5	0.976	0.736		
	4.6	0.846	0.614		
	7.6	0.717	0.508	0.727	0.524
	10.7	0.602	0.420		
	13.7	0.493	0.340		

The most interesting conclusion from these data is the small dependence of this fraction on the γ-ray energy between 660 and 2610 keV; for example, for the 10-cm disk source averaged over the 15.2-cm depth with an electronic cutoff of 150 keV, the values are 1.08 and 1.27, a difference of only 17%. In constrast, at 240 keV, this dependence is very large.

Influence of the soil-detector distance

For in-field measurements it is expected that an attempt will be made to keep the soil-detector distance a constant. A height of 6" from the soil to the frame that houses the detector and the shielding has been considered standard and this corresponds to 7.75" from the soil to the face of the plastic scintillator. However, due to limitations in the ability to control this height and the local variations in the soil surface, one must expect this height to vary. Therefore, the variation in the detector response for changes of about 3" in either direction has been computed.

The next table gives a tally of the fraction of the emitted γ rays of 660 and 2610 keV that give counts from 10- and 120-cm diameter sources for four soil-to-detector distances. In this case the values at the five depths have been averaged to give the value appropriate for a uniform distribution down to 15.2 cm or 6".

Source		Fraction of emitted γ rays depositing 150 keV in detector (%)			
Depth in soil (cm)	Diameter (cm)	Soil-detector distance =			
		4.75"	7.75"	9.06"	10.75"
		660 keV			
on surface	10	4.73	2.59	2.141	1.71
	120	1.06	0.90	0.834	0.75
uniform to 6"	10	2.14	1.28	1.081	0.89
	120	0.46	0.42	0.402	0.38
		2610 keV			
on surface	10	4.01	2.25	1.871	1.49

	120	0.98	0.81	0.744	0.67
uniform to 6"	10	2.44	1.49	1.266	1.04
	120	0.67	0.56	0.524	0.48

There are two interesting points about these results. First, from the reference distance of 7.75", a movement of 3" in either direction changes the result by less than a factor of 2.0, which means that for general surveys changes in the height of this magnitude are not crucial. (In the field there may be changes in the count rate from the natural background that would need to be accounted for before small changes in the count rate can be considered of interest, and the changes in the natural background may not be known, or even knowable.)

The second item of interest is that, in principle, one should be able to vary the detector height and obtain some information on the lateral extent of the source. For the smaller diameter source, in going from 10.75" to 4.75" the count rate increases be a factor of 2.4 or more. In contrast, for the larger diameter source this factor is 1.2 - 1.5. The former value reflects the change in solid angle of the detector from a point in or on the soil. For the latter case, this increase in solid angle as the detector is lowered is mostly compensated by the smaller viewing angle as defined by the detector shield. This result means that it may be useful to measure the count rate as a function of the detector height at strategic locations during in-field surveys to estimate the lateral extent of a source.

Measurement vs Modeled

The only method of testing the accuracy of the results from the modeling is to compare some calculated results with measured data. A spectrum was measured with a point source of ^{137}Cs, E_γ = 662.6 keV, and compared with modeled spectrum for a 10-cm diameter disk on the soil surface. From this measured spectrum, it was determined that 2.94% of the γ-rays emitted from this point source produced events in the spectrum above the electronic cutoff (estimated to be 150-keV). The corresponding value from the modeling is 2.64%, which is considered excellent agreement. This result suggests that one can simply scale the modeled values by 1.114 to obtain the best values.

Conversion of count rates to activity

In the next table, the source activities correspond to a measured count rate of 100 counts per second above an electronic cutoff of 150 keV. These values are based on the fractions of the emitted γ rays that are counted and include the 1.114 scaling factor deduced from the above measured value. It is suggested that this table might be useful for immediate in-field interpretation of the measured count rates. For the volume sources the values are given in the commonly used units of pCi/g and the values for surface sources are given in the less common units of pCi/cm^2. (If one assumes that a surface source were to be removed with the soil down to a depth of 0.67 cm (i.e., 1 g/cm^2), the activity in the removed soil would be the same value in pCi/g).

Source Depth in soil (cm)	Source Diameter (cm)	Units	Nuclide	Source activity Soil-detector distance 4.75"	7.75"	10.75"
on surface	10	pCi/cm^2	^{137}Cs	768	1403	2125
	120	pCi/cm^2	^{137}Cs	24	29	34
uniform to 6"	10	pCi/g	^{137}Cs	75	125	179
			^{228}Th	64	107	154
	120	pCi/g	^{137}Cs	2.4	2.6	2.9
			^{228}Th	2.0	2.2	2.5

It is clear from the data in this table that a count rate of 100 per second can corresponds to activity concentrations (i.e., in pCi/g) that range over a factor of greater than 10, depending on the lateral distribution; for example, for sources uniform to 6", from 2.9 pCi/g for a 120-cm diameter to 179pCi/g for 10-cm diameter. Therefore, the in-field interpretation of the data must involve, however crude, an estimate of the lateral activity distribution.

In the conversion from detector efficiency to radionuclide activity, one must consider the energies and intensities, or emission probabilities, for the γ rays for the specific radionuclide. Here we have considered ^{137}Cs and ^{228}Th. The nuclear data used for these two cases are given in the next table. Since ^{137}Cs has only one γ ray that is normally observable, it can be represented very accurately. In contrast, ^{228}Th and its daughters, which are assumed to be in equilibrium, have many γ rays. In our calculations for the above table, these have been represented by only three γ-ray energies, namely, 240, 660, and 2610 keV. This is expected to be sufficient because the γ rays are clustered near these energies and we have shown that the detector response to a large extent is independent of the γ-ray energy, at least, above 600 keV.

For ^{228}Th the γ rays with intensities (γ's per 100 decays) are given only where they are greater than 1.0%.

Nuclide	actual Energy (keV)	actual Intensity (%)	modeled Energy (keV)	modeled Intensity (%)
^{137}Cs	662	85	662	85
^{228}Th	74.8	10.5		
	75.0	1.3		
	77.1	17.7		
	84.3	1.2		
	87.2	6.3		
	238.6	43.6		
	240.8	3.9	240	53
	277.3	2.4		
	300.0	3.3		
	510.6	7.8		
	583.0	31.0		
	727.2	6.6	660	51
	785.5	1.1		
	860.3	4.3		
	1620.7	1.5		
	2614.3	35.9	2610	37

It should be emphasized that the background contributions to the count from the plastic scintillator must be subtracted from the measured data, before the activity is determined. For in-field measurements, this is not a simple matter. If the count rate from the activity of interest is not much larger than that from the background radiation, one must be concerned about the fact that the background will generally change with the detector position in a survey. Since the plastic scintillator can not distinguish the background counts from the nuclides of interest, the largest uncertainty in the activity profiles in the survey may be from the lack of knowledge about the background. Another version of this problem would occur if the idea of making measurements at different detector heights were implemented. Since the area of soil within the viewing angle changes with height, the background may change with the height.

CaF_2 detector

This detector system has been assembled especially to look for Pu isotopes and ^{241}Am by measuring the photon radiation around 16 keV, i.e., the L x rays from the decay of these isotopes, and at the 59-keV γ from ^{241}Am. In contrast to the plastic scintillator discussed above, the pulse-height, or energy, spectrum from the detector is obtained and then two specific portions (i.e., for the 16-keV L x rays and the 50-keV γ rays) can be counted in two scalers. The thickness of these

detectors was chosen to be quite thin (i..e., 0.152 cm) so they would stop most of the these low-energy radiations, but have most higher energy photons to pass through the detector without interacting.

The establishment of the relationship between the modeling for a CaF_2 detector and the measurements for this system has a complexity not present in the cases discussed above. The modeling has been done for a single 3" x 3" detector and the measurement system consists of six closely spaced 3"x3" detectors in a 2x3 array. Each detector generates a separate output pulse, but all of the outputs are mixed before the pulse-height is determined. Therefore, one has no information concerning the count rates in the individual detectors.

The CYLTRAN modeling calculations are summarized below. A 3"x3" square detector was modeled as a circular detector with a radius of 4.30 cm. These calculations determine the variation in the detector peak efficiency at a few photon energies as a function of the diameter of the source and its depth in the soil. It should be emphasized that for 16-keV photons the attenuation in the soil is such that the activity more than, say, 0.4 cm below the surface of the soil can not be seen by the detector. Therefore, this method can not be used to say the soil is clean, it can only say that the surface is clean.

Influence of depth in soil

The following table gives the relative peak count rate, or efficiency, for sources at different depths in the soil as a function of the source diameter for photons of 16 and 43 keV.

Photon energy (keV)	Source diameter (cm)	Soil-detector distance (cm)	Depth in soil (cm)	Relative peak count rate
16.0	10	10.55	0.0	≡1.000
			0.05	0.612
			0.15	0.233
			0.25	0.0852
			0.35	0.0347
			0.45	0.0118
16.0	60	10.55	0.0	≡1.000
			0.05	0.471
			0.15	0.140
			0.25	0.0413
			0.35	0.0129
			0.45	0.0039
43.0	30	18.18	0.0	≡1.000
			0.05	0.992
			0.15	0.886
			0.25	0.846

0.35	0.803
0.45	0.698
0.55	0.659
0.65	0.601
0.75	0.537
0.85	0.512
0.95	0.468

Influence of source diameter and source-detector distance

For 16-keV photons the peak efficiency has been computed for several source diameters and source-detector distances.

Source diameter (cm)	Soil-detector distance (cm)	Source depth =	Peak efficiency (%) on surface	uniform to 0.5 cm
10	10.55		3.086	0.603
30	10.55		0.612	0.0818
10	18.175		1.211	0.246
20	18.175		1.024	0.172
40	18.175		0.686	0.1213
60	18.175		0.441	0.0685
120	18.175		0.155	0.0209
10	25.80		0.605	0.127
60	25.80		0.318	0.0560
120	25.80		0.130	0.0201
10	33.42		0.361	0.0757
60	33.42		0.224	0.0402
120	33.42		0.110	0.0179

Influence of horizontal position of point source

The efficiency was modeled at 16 keV for a point source that was placed 18.175 cm from the detector and then displaced several distances away from the detector axis. This information has been used to estimate the efficiency for the array of six detectors. (In the array of six detectors, their centers are about 8.2 cm apart.)

Distance from axis (cm)	Efficiency (%)
0	1.25
8.2	0.95
12	0.72
16.5	0.50

Conversion of efficiency from one detector to six detectors

For a point source, the data in the above table can be used to determine the efficiency in each detector and these can be added to obtain the efficiency for the array. If the six detectors are arranged as

□ □ □
□ □ □, and the locations under the center of each detector is identified as

0 1 2 3
4 5 6

where "0" is a location outside of the array but at a distance equal to the interdetector spacing.

Source position	Efficiency for detectors 1 thru 6 (%)	Efficiency for array (%)
0	0.95, 0.50, 0.25, 0.7, 0.3, 0.2	2.9
1,3,4,6	1.25, 0.95, 0.5, 0.95, 0.7, 0.3	4.6
2,5	0.95, 1.25, 0.95, 0.7, 0.95, 0.7	5.5

For a source which is much larger than the size of the detector array (i.e., about 6"x9"), the efficiency will be essentially 6 times the value for a single detector. Some of the resulting efficiencies at 16 keV for the array of detector are as follows.

Source diameter (cm)	Source-soil distance (cm)	Source Source depth =	Efficiency for detector array (%) on surface	uniform to 0.5 cm
60	10.55		3.67	0.49
60	18.175		2.65	0.41
120	18.175		0.93	0.125

60	25.80	1.91	0.34
120	25.805	0.78	0.120
60	33.42	1.34	0.24
120	33.425	0.66	0.107

Conclusions

A great deal of experience has been gained this year in the area of in situ measurement of radionuclides with three different types of radiation detectors. By relating the modeling work with the detector development efforts and actual in situ measurements, we have been able to develop an understanding of the merits and limitations that are related to each type of detector system.

We have been successful in converting in-field measured detector count rates to soil contamination levels for data from three quite different detector systems, that is, a plastic scintillator, an array of CaF_2 detectors, and Ge semiconductor detectors. As illustrated in field surveys, these detectors systems each serve different and complementary purposes.

It is clear that any calculation of the contamination level, for example in pCi/g of soil, is only valid for a specific assumed spatial distribution of the radioactivity.

The modeling of the response of a CaF_2 detector has been used to provide contamination levels for plutonium and ^{241}Am. The modeling of the response of the plastic scintillator has allowing the conversion of large-area survey data to contamination levels of ^{137}Cs and results are available for similar surveys for ^{228}Th or ^{232}Th. The modeling of the response for the Ge detector has been used for determination of the contamination levels for plutonium and ^{137}Cs and would be available for measurements for many other radionuclides. These modeling calculations provide information on the influence on the counting rates from the distribution of the contamination in the soil, both laterally and with depth.

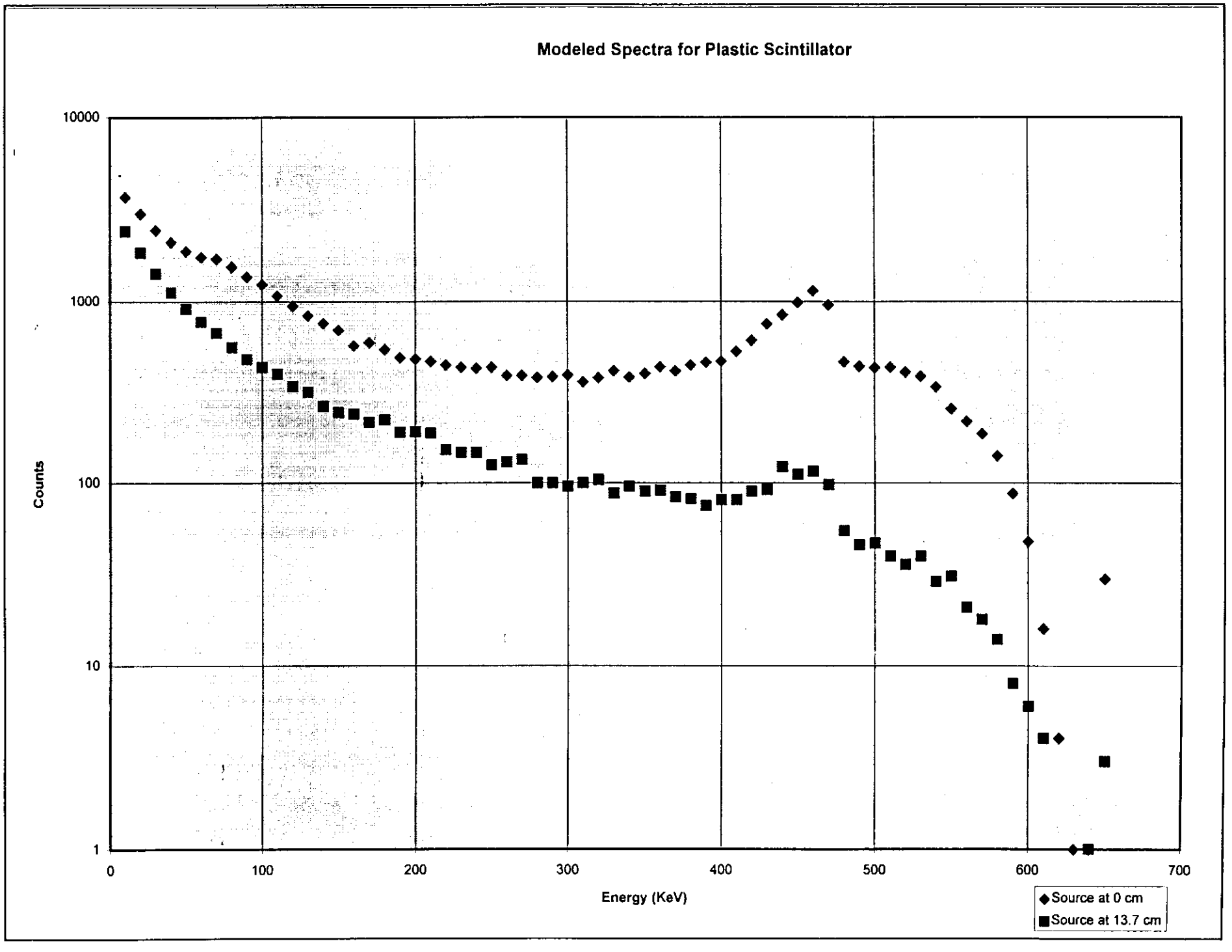
Modeled Spectra for Plastic Scintillator
10000
1000
100
10
1
Counts
0
100
200
300
400
500
600
700
Energy (KeV)
Source at 0 cm
Source at 13.7 cm